TURBOMACHINERY & PUMP SYMPOSIA | HOUSTON, TX
DECEMBER 14-16, 2021
SHORT COURSES: DECEMBER 13, 2021

FACTORS INFLUENCING THE ACCURACY OF TURBOMACHINERY AERODYNAMIC PERFORMANCE PREDICTIONS

Kurt Aikens
Aerodynamic Engineer
Siemens Energy
Olean, NY, USA

Scott MacWilliams
Manager, Development Testing
Siemens Energy
Olean, NY, USA

José Gilarranz
Manager, Packaging Technology
Siemens Energy
Houston, TX USA

James M. Sorokes
Principal Engineer / Engineering Fellow
Siemens Energy
Olean, NY, USA

Viktor Hermes
Key Expert, Aerodynamics
Siemens Energy
Duisburg, Germany

Kurt Aikens is an Aerodynamics Engineer in the Core Technology-Aerodynamics group. He earned a Ph.D. in Aerodynamics from Purdue University in 2014, taught Physics and Engineering for five years at Houghton College, and joined Siemens (now Siemens Energy) in his present role in 2019. His work focuses on aerodynamics research and development for centrifugal compressors. This has included new impeller development projects, development of analysis tools for advanced seals, support for development of internal performance prediction tools, and computational fluid dynamics support for customer centrifugal compressors and new component development testing.

José L. Gilarranz started his career at Dresser-Rand, now Siemens Energy, as a Senior Development and Aero/Thermo Engineer in 2002. Dr. Gilarranz is currently the manager of the Packaging Technology Team within the Technology and Innovation Organization. Prior to this he held several roles within the Global Operations and in the Sales Organization, including Manager for Technology Development & Commercialization of the DATUM ICS & Subsea Compression Product lines where he served as the main technical/commercial contact between Dresser-Rand and its clients in the area of compact compression systems. Prior to joining Dresser-Rand, he worked as a Rotating Equipment Engineer for Lagoven S. A. (now PDVSA) in Maracaibo, Venezuela.

Dr. Gilarranz received a B.S. in Mechanical Engineering (1993) from the Universidad Simón Bolívar and a M.S. (1998) and Ph.D. (2001) in Aerospace Engineering from Texas A&M University. He is a member of ASME and AIAA. He has authored or co-authored twenty-five technical papers & fifteen US Patents.

Viktor Hermes is a senior key aerodynamics expert with Siemens-Energy. He joined Siemens in Duisburg in 2012 as R&D Engineer in Core Technology Aerodynamics group. He previously worked for the RWTH Aachen University as CFD specialist. He holds a Ph.D. in Aerospace Engineering from RWTH Aachen University and is author and co-author of several technical papers and patents.

His current responsibilities include new product and component development (axial and centrifugal compressors); aerodynamic design, analysis, optimization and reviews; testing and troubleshooting.

Scott MacWilliams is a manager of the Development Testing at the Olean location of Siemens-Energy (formerly Dresser-Rand). He is a 1994 graduate of The University at Buffalo with a B.S. in Mechanical Engineering. He began his career with Dresser-Rand in 1995 as a Tooling Designer, which quickly transitioned to Rotor Center Manufacturing Engineer lasting for 9 years. Following that he became the Final Assembly Manufacturing Engineer in 2006. In 2008 Scott was promoted to General Foreman for the main Assembly and Packaging areas. In 2010 he moved to a Project Engineering role for Development Testing, responsible for execution of the assembly and testing of development projects at the Olean Operations. In 2015 Scott was promoted to the Manager of Development Testing in Olean. In this role he manages the development test technician and engineers supporting development testing as well as the overall responsibility for development testing that occurs at the Olean facility.

James M. "Jim" Sorokes is a Principal Engineer with Siemens-Energy with 45 years of experience in the turbomachinery industry. Jim first joined Dresser-Clark after graduating from St. Bonaventure University in 1976. He spent 28 years in the Aerodynamics Group, became the Supervisor of Aerodynamics in 1984 and was promoted to Manager of Aero/Thermo Design Engineering in 2001. While in the Aerodynamics Group, his primary responsibilities included the development, design, and analysis of all aerodynamic components of centrifugal compressors. In 2004, Jim was named Manager of Development Engineering whereupon he became involved in all aspects of new product development and product upgrades. In 2005, Jim was promoted to principal engineer responsible for various projects related to compressor development and testing. He is also heavily involved in mentoring and training in the field of aerodynamic design, analysis and testing.

Jim is a member of ASME and the ASME Turbomachinery Committee. He has authored or co-authored more than 60 technical papers / articles and has instructed seminars and tutorials at Texas A&M and Dresser-Rand. He holds several U.S. patents. He was elected an ASME Fellow in 2008 and was also selected as a Dresser-Rand Engineering Fellow in 2015. He was given a Lifetime Achievement award by Hydrocarbon Processing magazine in 2019.

ABSTRACT

This ***tutorial*** delves into the factors that impact the accuracy of turbomachinery performance predictions. The discussion is broken down into three parts… the influence of engineering tools / procedures, the impact of the various manufacturing processes and the uncertainties associated with performance testing. Under the engineering portion, the discussion focuses on the inaccuracies that can result from modeling assumptions or the computational methods themselves. The manufacturing segment explains how construction or machining techniques can yield parts that vary from the designs provided by engineering. Finally, the test portion provides an overview of the uncertainties associated with test methods, procedures, and instrumentation. The objective of the tutorial is to give readers a better appreciation of the role each of these considerations play in the prediction accuracy.

INTRODUCTION

Turbomachinery OEMs (original equipment manufacturers) are required to meet standard API tolerances on horsepower, discharge pressure, head level, rise-to-surge, surge margin, operating speed, and other performance parameters. For example, tolerances of ±4% based on the quoted horsepower and ±2% on discharge pressure are typically the standard. However, it has become increasingly common for end users to request more stringent tolerances on the performance guarantees. This is driven by a need to ensure that the new turbo-equipment will perform as expected in the end user's process.

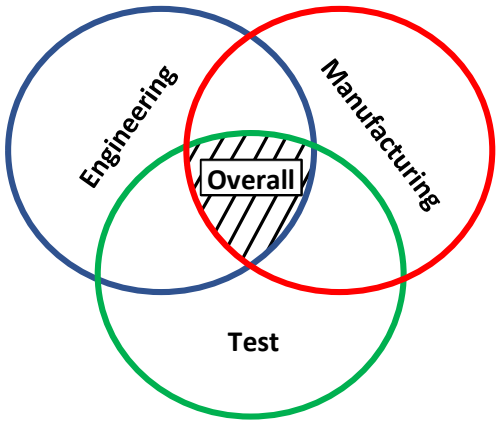

Figure 1. Factors influencing overall prediction accuracy

As shown in Figure 1, three keys to meeting the performance tolerances are: (1) generating accurate performance predictions based on results from the engineering design process; (2) manufacturing components accurately and precisely; and (3) performing final performance tests that accurately represent the field conditions. The overall accuracy is dependent on all three and cannot be better than

the worst of the three. For example, if the test data has an error band of ±2%, one cannot expect the overall accuracy to consistently be less than 2%.

Numerous factors impact an OEM's ability to accurately predict the performance of a turbo-compressor. These include the various tools used by engineers to generate designs and the analytical tools used to calculate the expected performance of the new designs. One also must consider potential variations due to disparities in the skills / experiences of the engineers using the tools. Manufacturing accuracy is of equal importance. Because predictions are almost exclusively based on drawing dimensions, any deviations from the drawings or solid models cause the performance to deviate from the performance prediction. Also, like the varying skillsets of the engineers, the variation in machine tool capabilities, machine tool operators and joining methods can play a role in the consistency of parts. Finally, when a compressor is tested to determine how well it performs relative to the prediction, there are various sources of error, including instrumentation accuracy, inconsistencies due to variation in test piping and/or test set up, differences in test methods / procedures used by OEMs, deviations in gas properties, or other operating parameters (as allowed by ASME PTC-10), etc. While these are not a part of the prediction process, they do directly impact the assessment of the prediction accuracy.

Each of these three key areas will be addressed in separate sections of this paper. The presentation order will be the same as that used in practice, with the impact of engineering being addressed first. One must design the parts before they can be manufactured, or more importantly, manufactured and assembled correctly. Therefore, manufacturing considerations are presented second. Finally, once the machine is assembled, it is tested to ensure it meets the end user's requirements, so, logically, test considerations are addressed last. Comments are offered on the relative contributions of engineering, manufacturing, and test methods/equipment to agreement between test results and the prediction, which ultimately is how once assesses the accuracy of the prediction.

Note: Though the paper focuses primarily on aerodynamic performance, comments will also be offered on how these key areas also apply to the mechanical performance of the compressor, i.e., rotor dynamics, stress levels, fatigue, etc.

ENGINEERING CONSIDERATIONS

Compressor Selection Process

One of the first sources of uncertainty in the engineering process is in the procedure used by proposal engineers to select compressor components for a client application. All compressor OEMs have some form of "stage-stacking tool" which they use to select the hardware that will be assembled to meet a client's specifications. Many of these have an embedded performance modeling tool that calculates the individual stage performance maps. Others are tied to a sophisticated database that contains the performance data for the OEM's product offerings. In the latter case, the information in the database might be for specific Machine Mach numbers and the selection tool will interpolate between those Mach number specific performance maps to estimate the performance at specified conditions. This interpolation process will introduce inaccuracy in the prediction. In addition, some OEMs apply efficiency and head coefficient correction factors during the selection process to:

- Account for variations in diameter (i.e., the database or performance model might only contain data for a so-called nominal diameter),
- Adjust the values obtained from the database or the embedded models based on prior test results for given stages,
- Adjust for stationary components that might not be optimally-sized for the given application, etc.

All of these factors introduce uncertainty into the compressor maps that are provided to the client in the proposal phase. Further, once the order is received, the OEMs order execution engineering team might make additional adjustments, including possible selection changes to ensure that the guarantees are met. These alterations introduce additional differences between the "as sold" performance and the "as expected" performance, which in turn, due to factors discussed in the remainder of this paper, will be different than the "as built" performance.

To minimize the potential prediction discrepancies, OEMs continually update the databases and/or embedded performance models used in their stage-stacking tool based on available test results from the stages in their product offerings.

1D Design / Analysis

One-dimensional design analysis is often one of the first tools that is used in the component design process due to its simplicity and speed. So-called "1-D codes" can be very useful early in the stage design process and for "what-if" analyses and/or scoping studies. For example, one-dimensional tools are quite capable when it comes to answering questions like, "How much would one need to increase the impeller diameter to increase the head (or discharge pressure) by a factor of X?" This section will describe the fundamental theory used by one-dimensional tools, and their resulting strengths and weaknesses.

One-dimensional tools rely on the Euler turbomachinery equation:

$$\Delta h_t = U_2 C_{\theta 2} - U_1 C_{\theta 1}, \quad (1)$$

where Δh_t is the change in total enthalpy of the fluid (directly related to the pressure rise) and subscripts 1 and 2 represent the quantities at the blade leading and trailing edges, respectively. Furthermore, U is the circumferential speed of the impeller at each location and C_θ is the circumferential component of the gas velocity in the stationary reference frame. As this is the fundamental theory that one-dimensional tools are based on, one downside of this approach is immediately apparent: Equation (1) only depends on information at the leading and trailing edges of the blades. Geometric information about the inner regions of the flow passage – information that includes blade angle and thickness distributions, hub and shroud contours, etc. – is not directly taken into account, though it does have a strong influence on the performance of the stage.

To use Equation (1) for performance predictions, additional simplifications are required. First, velocity triangles are used at the leading and trailing edges of the blades. See Figure 2 for an idealized example of the velocity triangle at the trailing edge. In this diagram, $\vec{W}$ is the gas velocity vector relative to the blade, $\vec{U_2}$ is the velocity of the blade tip, and $\vec{C}$ is the gas velocity vector in the stationary reference frame. By making a quasi-one-dimensional flow assumption, an expression for the magnitude of C_R, the radial velocity component of the gas, can be developed. Building on this, if it is assumed that the gas leaves the blade at an angle equal to that of the blade, β_2, expressions can be developed for $C_{\theta 2}$ and the flow angle, α_2. The former is useful for pressure rise predictions via Equation (1), and the latter can be used for specifying the diffuser geometry (e.g., pinch, vane setting angle). However, a variety of assumptions have been made to get to this point.

To determine C_R using the quasi-one-dimensional mass flow equation, for example, the area at the exit of each impeller passage is required. This can be approximated by using the exit width of the impeller and subtracting the area blocked by the blades themselves. However, this neglects the effective area reduction due to fluid dynamic effects. In the relative reference frame, the gas slows near the surfaces of the blades, the hub, and the shroud (if applicable) forming boundary layers that cause additional "aerodynamic blockage". Near the design flow coefficient, the blockage resulting from the thickness of the boundary layers is at a minimum, and reasonable performance predictions can often be attained. At off-design conditions, however, low momentum and/or separated regions can develop in the flow field, increasing the effective blockage. This leads to a need for complicated modeling schemes to rectify the one-dimensional tool predictions of speed line performance results, and high-quality test data are required to calibrate these complex exit models. It should be noted that a resulting side-effect of this is that off-design predictions from one-dimensional tools have inherently higher uncertainties. With the increasing regularity of off-design guarantee points for customer contracts, it is expected that test non-conformities will increase in turn.

An additional assumption mentioned previously, is that the flow exactly follows the blade angle, β_2, at the trailing edge. This is not perfectly accurate. In practice, the flow "slips", with $\vec{W}$ angled more toward the right of Figure 2. This is depicted in Figure 3. As is clear, $C_{\theta 2}$ decreases and the actual head rise (see Equation (1)) decreases. Having more blades in a given impeller can reduce the amount of slip but does not eliminate the effect entirely and adding more impeller blades reduces the passage area and the swallowing capacity. A model or correlation to address this "slip" or exit flow angle deviation is required and it directly impacts the predicted pressure rise for the stage.

Numerous slip correlations have been developed for 1-D tools, i.e., Weisner-Buseman, Eckardt and others (Japikse, 1996). These correlations account for various geometric aspects of the impeller design, but none are totally infallible. As a result, these correlations inherently lead to uncertainties in the 1-D predictions for impeller exit flow conditions. Improvements can be achieved by calibrating the correlations using detailed test measurements, but this can be a painstaking process as it must be done for each unique style of impeller.

One other major shortcoming of 1-D tools is that they fail to account for the three-dimensional nature of the flow through centrifugal stages (as suggested by the name 1-D). For example, it is well-known that the exit flow angle of a high flow coefficient impeller can be vary from hub to shroud by 10° or more with the flow angle along the shroud typically being more tangential than the angle along the hub. This skewed flow angle distribution continues into the diffuser where it could lead to varying incidence on diffuser vanes from hub to shroud and additional diffuser losses. Such effects will not be captured in 1-D tools. It might be possible to approximate the impact using further data correlations but as with the slip correlations, the results will still be approximate, and the accuracy of the 1-D based predictions will be impacted.

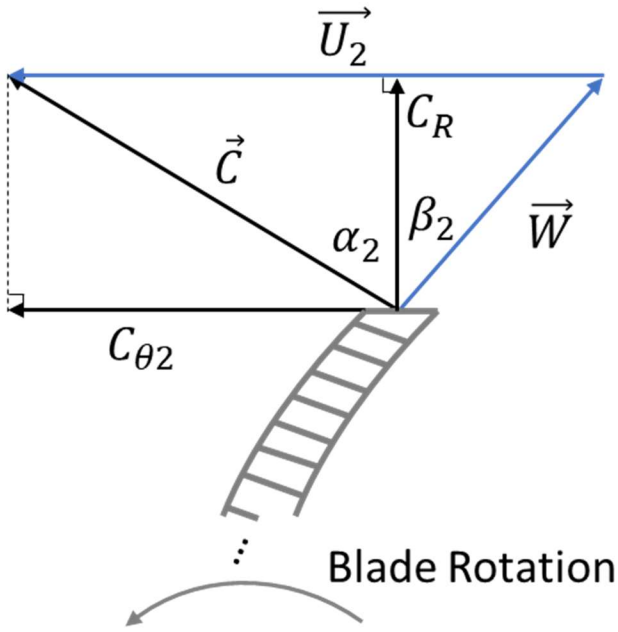

Figure 2. Velocity triangle diagram at the trailing edge (i.e., station 2) of an impeller blade in the ideal case.

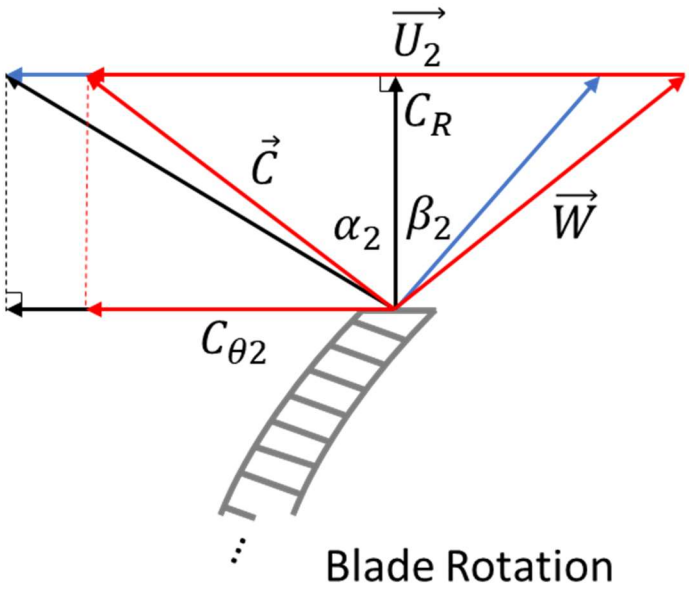

Figure 3. Velocity triangle diagram at the trailing edge (i.e., station 2) of an impeller blade. This diagram differs from that in Figure 1 because non-zero slip has been assumed – the relative velocity vector $\vec{W}$ does not follow the blade angle at the trailing edge exactly.

In addition to assumptions about blockage and slip effects, more sophisticated one-dimensional tools include models for effects such as disk friction, leakage, losses due to the tip flow for unshrouded impellers, recirculation losses, losses due to flow choking at overload, etc. (see Japikse, 1996, Aungier, 2000). With each additional model or correlation, more modeling parameters, or "knobs to turn", are added. When it is possible to tune these parameters using accurate results from other analysis methods (e.g., CFD, experiments, contract test data), the accuracy of one-dimensional methods can be excellent. However, the methods are only as accurate as the information that is used to tune them. Furthermore, as these models are often based on past data and experiences, users can unknowingly deviate outside of the range of applicability for these models when attempting to develop new stages.

Geometry Generation / Solid Model Development

Once the 1-D work is completed, the next step in the typical design process is to complete the hub and shroud profiles and generate the blade shape so that more detailed aerodynamic analyses can be performed. There are numerous commercial software packages available,

and many OEMs have their own proprietary systems for completing this process. It is not the purpose of this tutorial to do a thorough review of the available systems. Rather, it is to point out that the geometry generation exercise can lead to geometric uncertainties that can impact the performance prediction accuracy.

Virtually all of the geometry generation systems rely on various types of curve fits (i.e., Bezier polynomials, splines, various algebraic equations, etc.) when creating the various surfaces that generate the hub, shroud, and blade profiles. The output from these systems is typically an array of points or a collection of lines in space that are transferred to a CAD (computer-aided design) system so that solid models and drawings can be created, which are, in turn, used by N/C programmers to develop the machining instructions needed to manufacture the parts (Crouse & Sorokes, 1990).

Errors or deviations can occur if the software systems used by engineering, drafting and manufacturing use different techniques for modeling the geometry. For example, if the engineering software models the geometry using Bezier polynomials and the N/C system requires equivalent combinations of lines and circles, there will be some level of deviations between what was created by engineering and what is built by manufacturing. Steps are taken to minimize these discrepancies, but there are discrepancies, nonetheless. Likewise, if the engineering and drafting systems apply different curve-fitting methods, there will be deviations between the engineering and drafting geometries.

3D Analysis

In the past several decades the use of Reynolds Averaged Navier Stokes (RANS)-based CFD simulations for compressor performance predictions has increased significantly. The major motivation for this trend is that CFD is capable of simulating the three-dimensional flow field through a stage. As such, it can help to reduce development costs by virtual prototyping, and it is helpful for examining possible causes for compressor performance shortfalls.

In stage development work, following on results from simpler one-dimensional (and in some cases two-dimensional) design and analysis, CFD simulations of a single stage (impeller, diffuser, and sometimes return bend/channel) are often performed to assess the impact of more detailed geometry variations. This allows designers to vary aspects such as the blade incidence at the leading edge, blade angle distributions, hub/shroud contours, etc., and gauge how the stage performance responds to these modifications. Subsequently, geometries with the highest potential are subsequently experimentally tested to more accurately gauge performance.

Beyond analyses at the component and stage level, RANS-based CFD is sometimes used to analyze the flow in multi-stage configurations. However, this type of analysis is performed quite rarely because compressor OEMs rely heavily on experience-based and validated component design rules during order execution and because of the time/resources required to complete such a complex analysis. However, for new stages or components that fall outside the OEM's experience and for compressors that are short in performance or show other non-conformances, CFD is the tool of choice because it is relatively fast and provides high-quality insight into the component or stage performance of the as-build geometry.

Although RANS based CFD has advantages compared to one-dimensional tools and tests and is widely used, there are some sources that contribute to the uncertainty of its results. Major contributors are uncertainties related to geometry simplification, the impact of turbulence models, and proper rotor-stator interface selection. Furthermore, computational mesh resolution affects the results. It is, however, not very time-consuming nor complicated to perform a mesh sensitivity study and estimate this impact (discretization error) on the results, which should be performed for each new configuration (Denton, 2010).

In contrast, the impact of geometry simplification cannot be assessed in a simple, systematic way. Ultimately, it is a trade-off between increasing effort and uncertainty reduction. For example, in CFD simulations of intermediate stage configurations, secondary flow features like the shroud and hub cavity flows are often neglected, and just the main flow path is part of the simulation. The cross-section of an impeller with the secondary passages highlighted is given in Figure 4. These flow paths are often ignored because simulations of just the main flow path are more efficient. First, the CFD user does not have to extract the geometry of the secondary passages and the additional domains do not need to be meshed. So, the overall problem size is smaller which improves simulation run time and often the convergence behavior. The impact of the neglected secondary flow features can be assessed by using empirical models, and the CFD results of the simplified geometry can be corrected accordingly. Even if the secondary flow features are included in the simulation, however, there are still uncertainties related to the sealing gap size under operating conditions. The uncertainty here results from the combining of manufacturing tolerances, material behavior under rotational speed, etc. So, if the uncertainty level is almost identical for a configuration with secondary flow features compared to the one without, it is wise to just perform a main flow path simulation and correct for missing features. Uncertainties related to the third order effects like split line leakage are even more complicated to account for. Fortunately, these effects tend to be quite small.

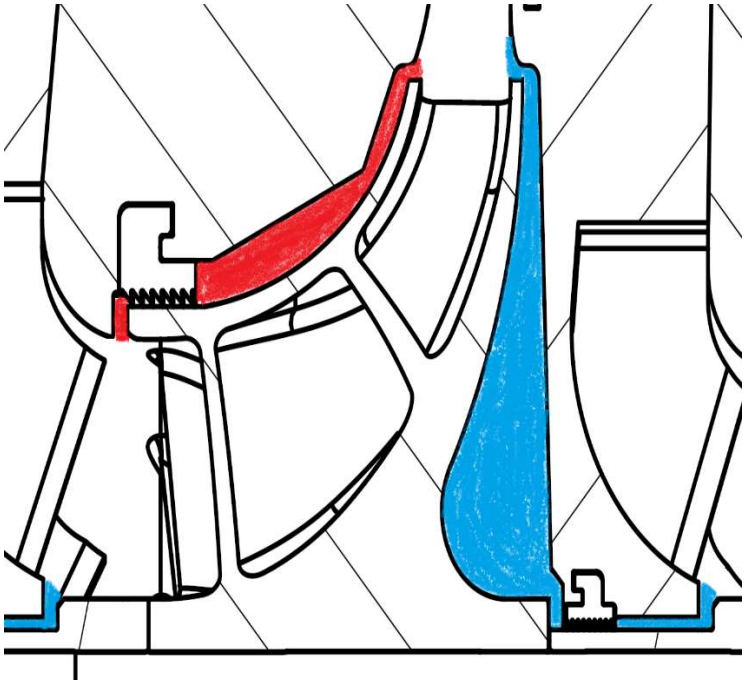

Figure 4. Cross-section of an impeller with the secondary flow passages highlighted. The hub-side cavity is colored blue, whereas the shroud-side cavity is indicated with red.

Related to geometric simplifications, the impact of surface roughness on performance predictions can be significant. Commercial CFD solvers include capabilities for modeling the impact of uniform sand grain roughness on the flow field. However, the surface roughness of manufactured components cannot always be reasonably approximated in this way. Furthermore, the roughness can sometimes vary in different parts of the machine and even a given component. An example of the impact of surface roughness on CFD polytropic efficiency results is shown in Figure 5. In this plot, the roughness was varied from the anticipated manufacturing roughness ("Roughness = 1x") to twice that value ("Roughness = 2x"). Not only does the stage efficiency (impeller and diffuser) decrease by about 1%, but the predicted surge point shifts as well.

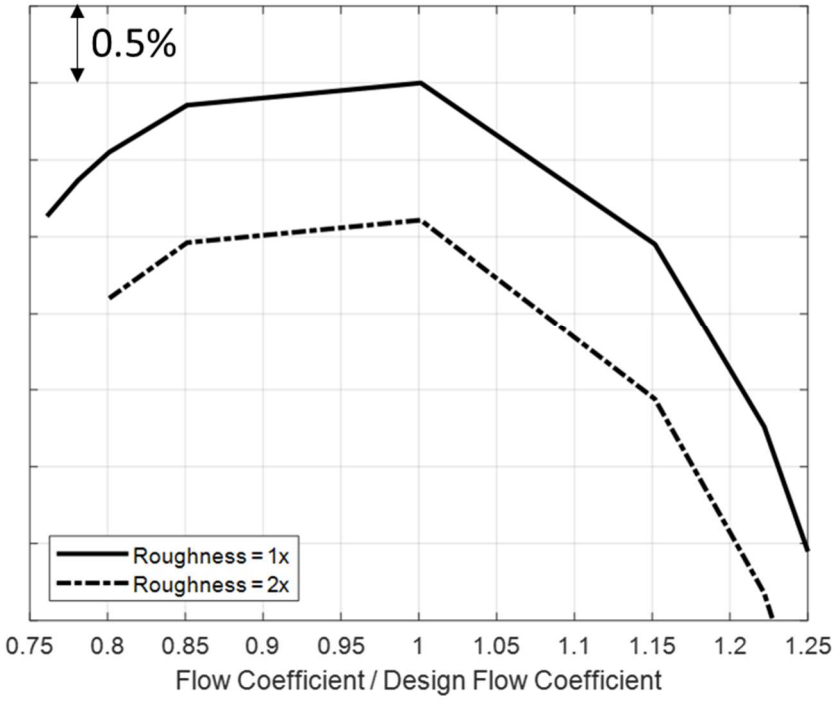

Figure 5. Polytropic efficiency results for a stage (impeller and diffuser) using two different specified wall roughness values.

Also influencing the ability of CFD to generate accurate performance predictions: the flow in turbomachinery components is turbulent. Because turbulence is by nature unsteady and multi-scale, steady-state simulations require a model that mimics the time-average effect of turbulence on the flow, the so-called turbulence model. There are many different turbulence models available and any commercial CFD solver offers at least a handful of them (Mangari & Mauni, 2011, Sorokes et al, 2016, Singh et al, 2017, Durbin, 2018). Different turbulence models are optimized for different flow topologies and tend to deviate in predicting the onset of flow separation, reattachment, and corner and tip vortices. Due to a high sensitivity of performance on actual flow in the component, the turbulence model is one of the major contributors to prediction uncertainty. As an example, consider the core stage (impeller and diffuser) efficiency predictions for two different impellers shown in Figure 6. Both the popular $k-\epsilon$ and SST turbulence models were used for each design, and the results are quite different. To clarify the results further, predictions for the benefit of the new impeller design relative to the original are shown in Table 1. The $k-\epsilon$ model predicts a 0.6% design point efficiency boost for the new design, with no reduction in the surge margin. The SST model, on the other hand, predicts a 1% efficiency boost with a 2% reduction in surge margin. This illustrates the uncertainty of performance predictions due to the choice of turbulence model. Our experience is that the selection of the best turbulence model is very case-dependent, and an experimental validation is extremely valuable. Theoretically, higher fidelity CFD models like large-eddy simulations (LES) or direct numerical simulations (DNS) resolve a larger portion of the turbulence spectrum instead of modeling it. But these CFD methods pose significantly higher requirements on the utilized hardware and lead to significantly higher simulation run times. They are seldomly used in industry, and if they are, they are only used for very small physical domains like blade cooling holes or ejectors.

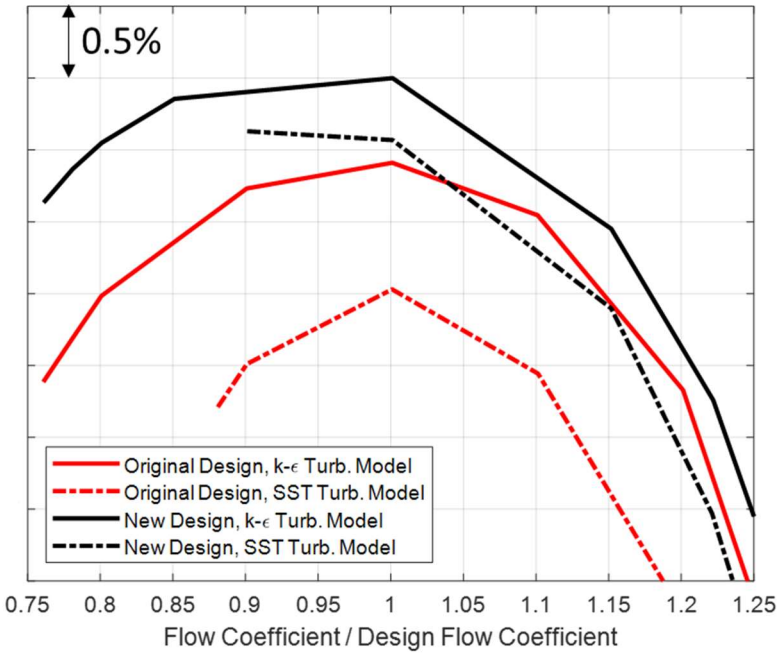

Figure 6. CFD-calculated polytropic efficiency curves for two impeller designs (the "original design" and "new design") near the design flow coefficient.

Table 1. Tabulated design point efficiency and surge margin results from Figure 6. Efficiency and surge margin benefits are the difference between the new and original designs for each impeller design, independently calculated for both turbulence models.

Case	Relative Design Point Efficiency	Efficiency Benefit	Surge Margin	Surge Margin Benefit
Original Design, k-e	99.4%	--	24%	--
Original Design, SST	98.5%	--	12%	--
New Design, k-e	100.0%	0.6%	24%	0%
New Design, SST	99.6%	1.0%	10%	-2%

An additional uncertainty with CFD is the choice of rotor-stator interfaces. A mixing plane interface is a default choice for RANS simulations with rotating and stationary components. An example that highlights how the flow is averaged in the circumferential

direction is shown in Figure 7. This interface methodology works well in many cases because it removes the influence of the relative position of rotor and stator components. The weakness of the mixing plane approach, however, is observed for configurations with closely-coupled components, like vaned diffusers where the vane leading edge is very close to the impeller trailing edge. If the distance between components is too small, or if the interface is located in an unmixed wake or in the upstream potential field of a vane or blade, the CFD result in the corresponding domain is influenced by the presence of the interface. Because conservative variables are averaged in the circumference by the mixing plane approach, gradients disappear and averaged, artificially homogeneous conditions are present on the other side of the interface. The impact on the simulation results is, thus, comparable to a situation with boundaries placed too close to regions with high gradients – an inappropriate constant-value boundary condition is being specified, which completely dominates the flow field near the blades and/or vanes.

A transient simulation, which assumes that the flow field at the interface is time dependent, is the method of choice for such close-coupled configurations. The drawback of transient simulations, in contrast to steady-state, is that the simulation time increases by a factor of 10 to 100. Application of harmonic methods, which have been available in all turbomachinery-specific commercial solvers for several years, reduce the factor to 3 to 5. This is acceptable for application in industry. A sensitivity study on the impact of the interface and/or its location is recommended for configurations with small distances between components.

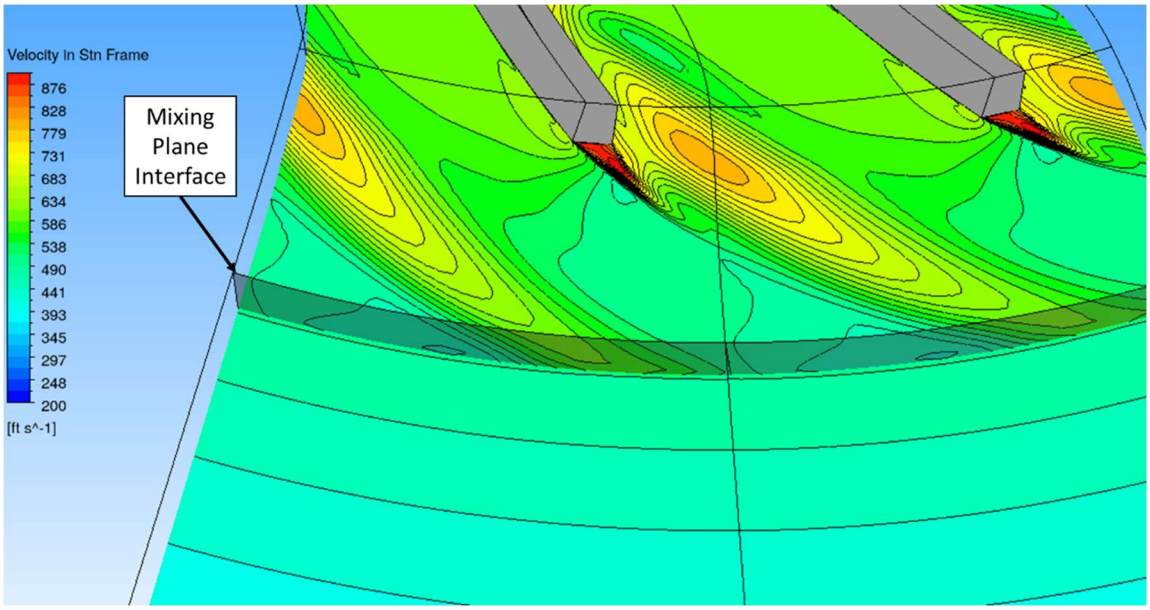

Figure 7. Illustration of mixing plane interface, showing the circumferentially-averaged flow velocity downstream of the impeller blades.

Finally, while it may seem obvious, it should be noted that care must be taken to ensure simulation convergence. Convergence history plots (e.g., residuals, other quantities of interest) can be used to assess the steadiness level of the solution and gauge whether the simulation has converged. Specifically, compressor efficiency should be monitored during the simulation, as it tends to be the most sensitive performance value.

Despite the challenges associated with CFD, it is an invaluable tool for compressor OEMs. Some of the difficulties can be mitigated by thoroughly documenting past experiences and creating best practices for frequently reoccurring CFD tasks. Additionally, systematic mesh and sensitivity studies increase the confidence in CFD results and help to identify their uncertainties for the corresponding configuration. Comparison with accurate and reliable test data and fine tuning of CFD setups can lead to accuracy of CFD results within a few percent for well-known, reoccurring CFD tasks at design flow conditions. At deep off-design, uncertainties are significantly higher, which hinders a reliable and accurate prediction of the surge limit, for example. Despite the difficulties of CFD to predict absolute performance and range value, it is very well suited to predict the correct trends in the performance results between two competing designs.

MANUFACTURING CONSIDERATIONS

Even if engineering designs and the associated performance predictions are perfect in and of themselves, if parts are not manufactured and assembled accurately, the actual machine performance will not agree with the engineering prediction. It is vitally important to recognize that virtually all engineering predictions are based on the drawing and/or solid model dimensions. If the dimensions of the component parts and assemblies deviate from the drawing or solid model geometries, the performance will deviate from the prediction. This is true for any and all predictions related to aerodynamics, rotor dynamics, stress levels, natural frequencies, part life, or any other aspect of the turbomachine's performance.

In considering manufacturing's impact on prediction accuracy, it can be divided into four basic categories: (1) machining, (2) castings / additive manufacturing, (3) joining, and (4) assembly. Each will be addressed in the section that follows.

Machining

It is well-recognized that machine tools or other methods of machining (i.e., electro-discharge machining or EDM) result in some level of inaccuracy between the finished part and the engineering drawing or model.

Mills, Lathes, Drills

Most machine tool manufacturers provide an estimate of the accuracy of their mills, lathes, drills and the like based on the assumption that the machines are properly maintained and overhauled on a regular basis. It is also critical that the "feeds and speeds" are kept within specified limits for the material being machined and that the cutters, drill bits, etc. are sharp and properly installed. If all of those conditions are met, a mill, lathe or drill will likely have an optimum accuracy of ±0.005" (0.127mm). However, as the bearings or other joints in the machine begin to wear… as the cutters or drill bits become dull… as the feeds and speeds are pushed outside specified limits to increase production, the geometric accuracy will degrade. The ±0.005" (0.127mm) tolerance might become ±0.010" (0.254mm) or even 0.020" (0.508mm) or worse if the machine is poorly maintained or if dull cutters are used. While these numbers might appear small, they can represent a large percentage of the aerodynamic flow path height in low flow coefficient stages, where impeller and diffuser passages heights can be 0.070" (1.778mm) or smaller!

Tool pressure on parts can cause further deformations, i.e., bending thin blades or vanes due to the cutter force or because of the heat input into the part as a result of the cutting process. This is one area where it is important that the manufacturing engineers educate the design engineers as to the capability of the machine tools. While the aerodynamic design engineer might desire very thin blades, they must understand the manufacturing challenges faced to achieve such and the probability that the final shapes will not match their designs simply because it is impossible or impractical to build such a thin blade.

One other possible discrepancy between the engineering prediction and the manufactured parts is the machining fillet radii in the corners between blades or vanes and the adjacent hub or shroud in the flow path (see Figure 8). If the part was engineered with a given radius in mind or with a sharp corner and a different cutter radius is used in production, there will be a difference in the passage area. If this difference is significant, it will impact the performance of the component and, therefore, the performance of the machine. There must be coordination between the design and manufacturing engineers so that both parties are aware of the corner radii that will be used in manufacturing the parts. If the design engineer requires that a specific corner radius be used, he/she must ensure that the manufacturing personnel are aware of this necessity. Otherwise, the manufacturing engineer will likely default to the next larger standard cutter radius, because the larger tool will allow the material to be removed faster.

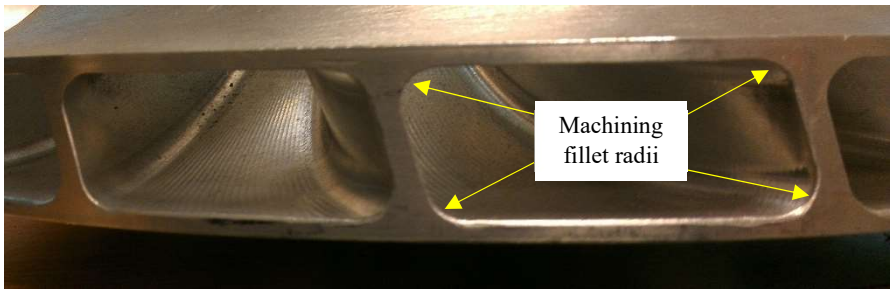

Figure 8 – Machining fillet radii in a single-piece milled impeller

EDM

Electro-discharge machining has proven to be a very effective method for removing material when it is not possible to do so with milling or other machining processes, i.e., when it is not possible to have the "line of sight" necessary for conventional or even specialized cutters. Special electrodes can be shaped to reach into these areas to finish machine the flow path in impellers, return channels and the like. One factor that comes into play with EDM is the so-called re-cast layer, related to the heating of the material that occurred during the EDM process. The properties of the material change in this area, which can impact the mechanical integrity of the part. Therefore, steps are taken to remove the re-cast layer, but these remedial measures can result in geometric deviations from the engineering geometry that will impact the aerodynamic performance.

Casting / Additive Manufacturing

One important consideration on both cast and additive manufactured (3-D printed) parts is the geometric accuracy relative to the engineering specifications. Many different approaches can be used for both cast and "printed" parts. Some of these produce very accurate parts while others yield parts with greater geometric scatter. For example, some sand-casting approaches are characterized by

very wavy or pocked surfaces while ceramic core castings can provide geometric accuracies close to that from milling. Likewise, the accuracy of parts built via additive manufacturing can be suspect, or of very high quality, depending on the printing scheme being used.

Historically, one of the biggest drawbacks to cast or "printed" parts was the surface finish, which will be discussed in the section that follows. It is possible to correct the "as cast" or "as printed" surface finishes. It is also possible to account for the rough finishes during the engineering design / prediction process. To do so, the engineer must know in advance what the surface roughness will be on the finished part. If the engineer assumes a hydraulically smooth surface finish in his/her calculations because he/she assumes a certain method is being used, but a different method is applied resulting in a part that has a much rougher finish, there will be a discrepancy between the engineering prediction and the test results. Therefore, it is critically important that there is a feedback loop in place should the manufacturing team decide to change the method to be used in the order execution process.

Surface Finish

Surface finish can have a significant impact on prediction accuracy. As noted above, this is especially true in additive manufactured or cast parts because of the rough finishes in the "as cast" or "as printed" parts. However, it is also true when milling or turning flow path surfaces. Much has been written about the machining grooves or "serrations" that are often left on impeller blades or diffuser / return channel vanes as a result of the point milling process (see Figure 9). These "peaks" or "valleys" on the vane or blade surfaces are typically not considered during the engineering design process. Therefore, said "peaks" and "valleys" either represent: (a) reduced area (blockage) in the flow path because excess material was left on the surface or (b) excess area in the flow passage because of the removal of too much material or (c) roughly the correct area because the "peaks" and "valleys" average out. Regardless, the presence of the "peaks" and "valleys" is a departure from the geometry used when generating the engineering prediction.

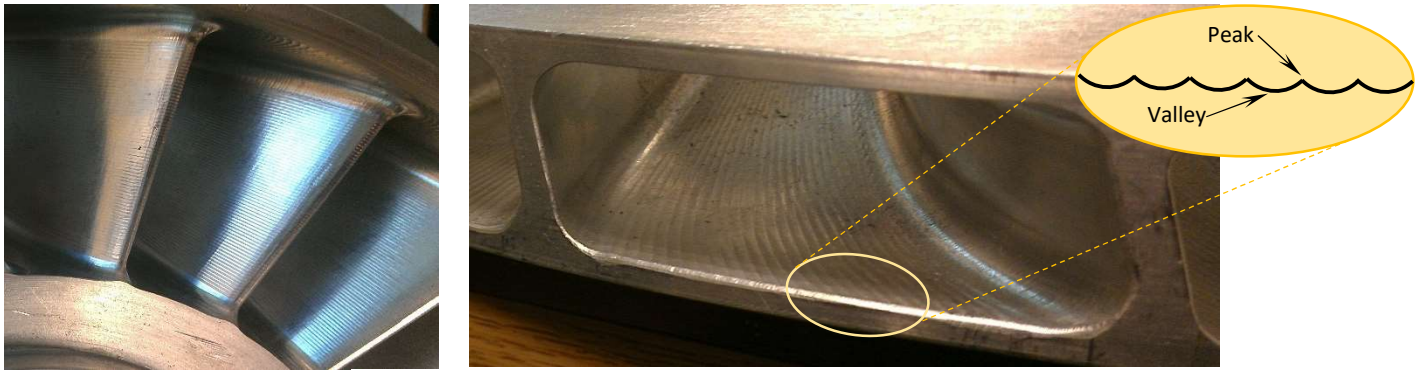

Figure 9 – Machining grooves created via point milling

Beyond the "peaks" and "valleys", the overall surface roughness of the part must be considered, in particular on cast or printed parts. Steps must be taken to bring the roughness as close as possible to those used in the engineering prediction process. If the prediction is based on a 63rms impeller flow path finish and the actual part has a 180 – 240rms finish, the efficiency can be 1.0 – 1.5 points lower for a 0.080 flow coefficient, 15" (381mm) impeller. Therefore, if necessary, the impeller or other stationary components can be extrude-honed, run through a slurry finish or even hand-polished. However, care must be taken that the finishing process does not remove too much material or damage the blade or vane leading edges. Removing too much material can impact the robustness or natural frequency of the part, leading to potential mechanical concerns. Damaged or misshapen leading edges can contribute to aerodynamic performance issues, causing the test results to deviate from the engineering prediction.

Joining Methods

The joining methods used to fabricate compressor components can have a wide range of influences on geometric accuracy. This is true for both rotating (impellers) and stationary components. From a very high level, the geometric inaccuracies tend to fall into two categories: area and/or surface shape deviations. Area issues are relatively easy to account for in the engineering design / analysis phase. The surface shape variations are much more difficult to model or assess via the typical analytical methods used. For example, it is difficult to accurately model in a CFD or FEA analysis the waviness of a wall that was designed to be flat. Said waviness might occur as a result of the joining method and might be very arbitrary in nature, making it impossible to measure and/or replicate analytically.

While many joining methods can be used, this paper will only focus on four: (1) fillet welding, (2) electron-beam welding, (3) brazing, and (4) bolting. These tend to be most popular methods in industrial turbomachinery. Please note that parts are also joined via rail fits, dove tails, J-grooves or the like but these will be addressed under the *Assembly* section to follow.

Fillet Welding

The most obvious deviation that fillet welding presents is the weld fillet itself. The fillets result in a reduction in the area of the component flow passage, which directly impacts the gas velocities and flow capacity. The most obvious issue that must be considered

is whether or not the weld fillets or the size of the weld fillets were included in the engineering design process. In the same way that the machining fillet size must be understood, the weld fillet size or presence must also be included in the engineering analyses if the prediction is to be accurate. The impact of the weld fillet blockage is of greatest concern in so-called three-piece welded impellers or milled-welded impellers because of the impact of the fillets on the impeller throat and exit areas (see Figure 10). As described by Frier et al (2020), excess blockage at the throat and exit can directly impact the impeller capacity and head-generating capability.

The other concern with fillet welded components is the heat input into the part during the welding process. This can cause residual stresses that might lead to deformations or distortions in the parts during the stress relief or heat-treating processes. These distortions can become large enough to impact the performance of impellers, vaned diffusers and return channels. For example, consider the impeller shown in Figure 11 below. The leading edge of the blade is supposed to be a straight line but due to distortion in heat treat, the blade leading edge is now slightly "S"-shaped. This means that the blade angles are not per the engineering specification, so there will be subtle differences between the predicted and actual performance.

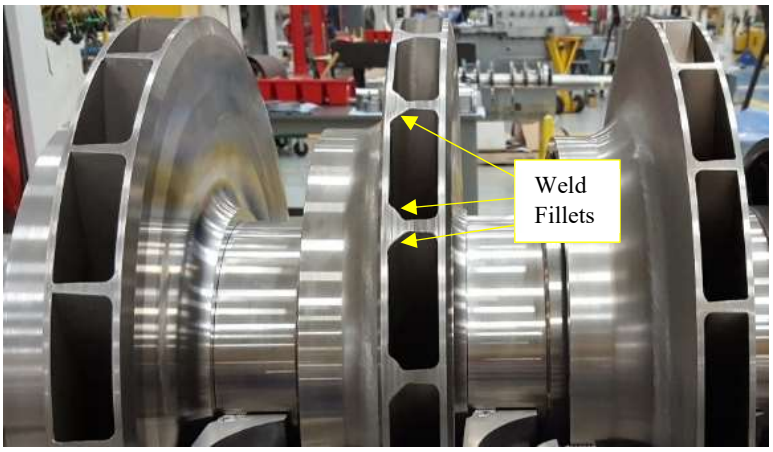

Figure 10 – Fillet welded impeller (center) compared to EB-welded impellers

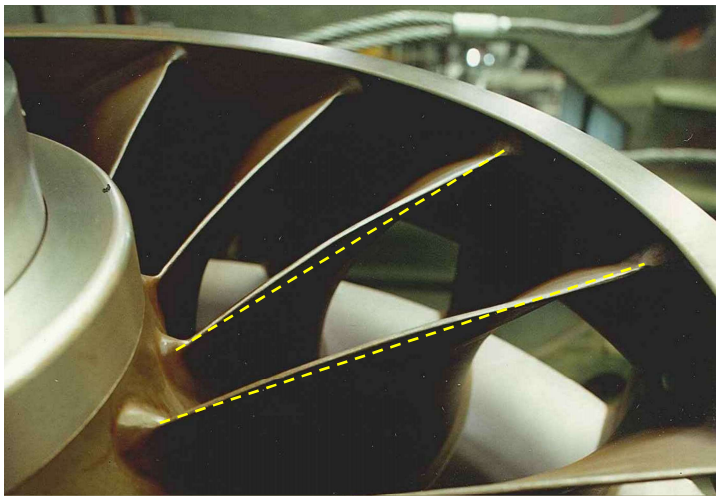

Figure 11– Example of blade leading edge distortion due to fillet welding and heat treatment

Another indirect impact of using the fillet welding process are the steps required to "clean up" the component after welding. There tends to be some level of weld "splatter" during the fillet welding process. Therefore, the part is typically grit-blasted or sand-blasted to remove this extraneous material. This can have a detrimental impact on the flow path surfaces, leading to concerns similar to those address in the *Machining* section above. As noted, if the surface finish after blasting does not conform to the finishes assumed in the engineering design process, errors between actual and prediction performance will occur. Likewise, care must be taken with any surface finish treatments that might be applied to ensure that the finish part conforms to the engineering design / models, i.e., that material thicknesses and blade / vane profiles are properly maintained.

Electron-beam welding & brazing

Electron-beam welding eliminates the "in-passage" fillet blockage, but it does still impart residual stresses in the component. This is particularly of concern for very low flow coefficient impellers that are often built via EB-welding. These residual stresses can lead to "dishing" or "potato-chipping" of the impeller (see Figure 12). Though exaggerated in the figure, these deformations can be large enough to cause misalignments between the impeller and the downstream diffuser. These misalignments can lead to premature stall, high frequency aerodynamic loading of the rotor system, or other phenomena that reduce the flow range of the compressor or compromise the mechanical behavior of the unit.

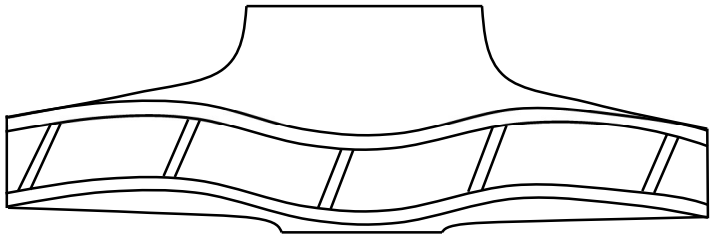

Figure 12 – Exaggerated schematic of "dishing" or "potato-chipping" of impeller

There are also limits on how thin of a blade can be EB-welded. When scaling a standard product offering to a small size, it is possible the scaled blade will be too thin to EB-weld. If the blade is "thickened" to allow EB-welding, the increased thickness will impact the area in the impeller, so the engineering prediction must account for the proper thickness. If it is not, the prediction will not be accurate, and the compressor will likely be low in capacity.

From a mechanical perspective, an EB-welded impeller has a small gap at the joint because the EB welded cannot extend across the full thickness of the blade (see Figure 13). This small gap can be a "stress riser" and will impact the robustness and natural frequencies of the impeller. If the engineering design assumed a complete joint, the mechanical characteristics of the actual impeller will be different than predicted by engineering. This can be addressed by using a brazing material during the eb-weld process, resulting in the so-called e-brazed joint.

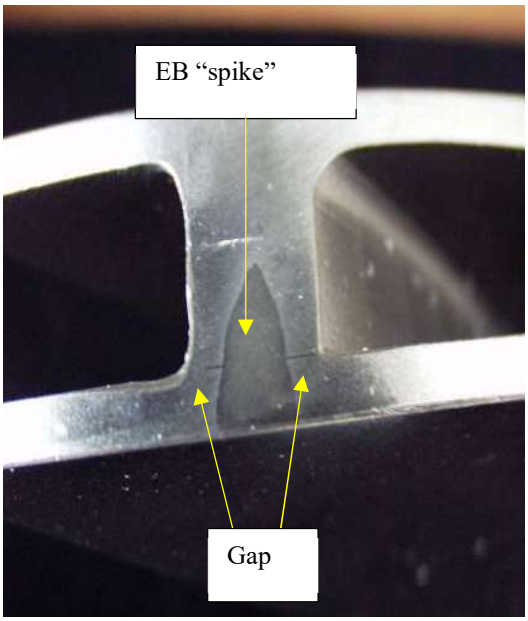

Figure 13 – Electron-beam welding joint illustrating gap on both sides of EB joint

Brazing eliminates most of the heat-input issues associated with the welding processes addressed above. There is still a minimum thickness requirement for brazing, similar to the limit cited in EB-welding, so the same issues might occur for small-scaled impellers or stationary components. "Dishing" or "potato-chipping" might also occur with brazed impellers.

Bolting

Bolting is not used for impellers, but it is commonplace in return channels. It eliminates the machining fillets on one side of the flow passage, so blockage is typically not an issue. The main concern with bolting is deformation or deflection of parts at load. Because bolting does not form a joint over the full length of the vanes (see Figure 14), parts can pivot or deflect, leading to misalignment of components. Care must be taken to make sure that the bolted assembly is sufficiently rigid and that the bolts provide sufficient strength to withstand the pressure loads during operation.

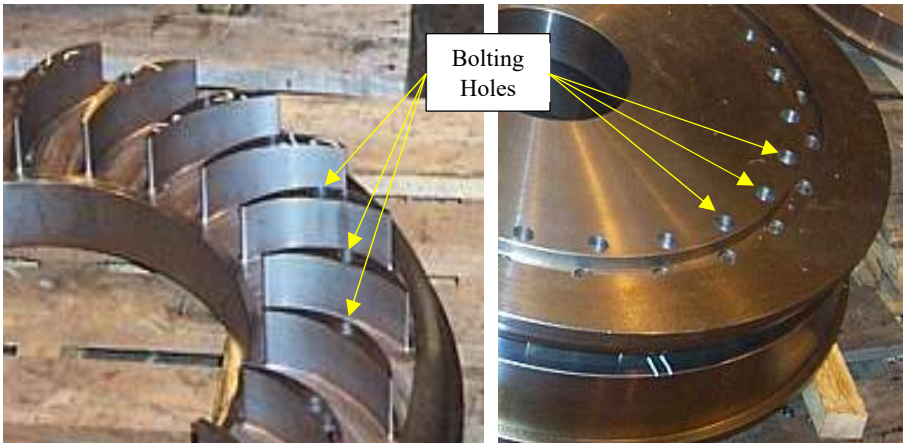

Figure 14 – Photos of bolted return channel – One bolt per return channel vane – Return channel vanes shown at left; assembled return channel at right

Assembly

As discussed above, there are potential sources of error or deviations in the manufacturing of individual components. However, additional errors are possible during the assembly of the compressor. Many of these are likely associated with deviations in the component parts but others will be associated with the clearances or other provisions that must be made to allow the assembly of the parts. While specification of zero clearance would be ideal, assembly of the compressor would be impractical, if not impossible. Because these allowances must be designed into the assembly process, they result in opportunities for parts to move during assembly or when the compressor is in operation. As described by Kocur and Sorokes (2019), bundle deflections due to tolerance stack-up or thermal growth will occur when the machine is operating at full-load and full-pressure. As their paper describes, these deflections can cause shifts in performance maps, reductions in operating range, lower performance, etc. All of their observations will not be repeated herein and those interested in the details should obtain a copy of that paper. However, one of the key points made in the paper is that the deflections can vary between Type 1 and Type 2 testing, resulting in differences in the performance maps derived from the two tests. In the example they referenced, the stall margin and efficiency level were different between the Type 1 and Type 2 tests due to the bundle deflection and the variation in division wall seal clearance between the two tests. The key takeaway here is that the same compressor tested under different conditions can yield different test results, which are compared to one engineering performance prediction. Because the test results are different, both cannot align well with one predicted curve.

This discussion could well have been included in the Test section which follows but the issues discussed above are more about the tolerance stack-up or assembly of the machine rather than some issue related to the test set-up, test loop, instrumentation, data acquisition system or the like.

Digging a bit deeper into assembly considerations, there are many seemingly innocuous assembly features that can lead to geometric deviations from the engineering models. Obvious examples are the rail fits, t-slots, or other similar assembly features for connecting parts. As noted, to permit such assemblies, there must be clearance around the surfaces of the fits. Granted, these clearances are typically very small but, if not manufactured properly or if damaged during repeated disassembly / re-assembly, they can lead to dimensional inaccuracies.

Assemblies must also account for potential deflections due to pressure loads or deformations due to thermal influences, i.e., thermal growth. Consider the installation of vaned diffusers. Said vanes are typically rail fit into or machined integral with one wall of the diffuser. The diffuser vanes are installed in the machine in the “cold” or room temperature condition. When the compressor pressurizes and heats up during operation, it is possible that the two diffuser walls will grow apart, creating a gap between the diffuser vane and the adjacent wall. Steps can be taken to eliminate the gap, but the diffuser width will still increase, leading to changes in the incidence angle on the diffuser vane leading edges as well as flow angles downstream of the diffuser vanes. Again, if the engineering predictions fail to account for these deformations / deflections, the prediction and test data will not agree.

Other factors that must be considered during assembly are the potential for rotor eccentricity, rotor sag and/or rotor float. Rotor eccentricity occurs when the rotor or rotor components (i.e., impellers, balance piston, division wall sleeve) are no longer centered between the adjacent labyrinth seals. This can occur as the rotor deflects in its various mode shapes or if the rotor sags in the center simply due to its own weight. To avoid potentially damaging rubs, the seal clearances must be adjusted to account for the rotor deflections or rotor sag. The variations in seal clearance from stage to stage or circumferentially cause performance variations, which again can be a source of error between the actual and predicted performance.

Rotor float is a term typically used to describe the rotor axial movement due to changing thrust loads as the compressor operates at different conditions across its performance map. The rotor movement, though small, can impact the physical alignment of the impeller and diffuser openings. If the movement is sufficient and if the diffuser entrance flaring does not account for this movement, the diffuser wall can obstruct the impeller exit flow, leading to premature stall or other adverse performance effects. Further information regarding this issue can be found in Sorokes and Kuzdzal (2020) and Kocur and Sorokes (2019). The key takeaway here is that the rotor is assembled into the compressor in the "cold" and zero speed condition, but the rotor can move axially during operation causing the impeller / diffuser alignment to deviate from the arrangement typically used for performance predictions.

One last assembly consideration that will be addressed is the horizontal split gap. In nearly all multi-stage, single shaft compressors, the stationary components are horizontally split to allow installation of the rotor (see Figure 15). Granted, there are exceptions… notably the OEM's legacy CBF product line… but the vast majority of OEMs use a horizontally-split bundle or case concept. This leads to two sources of deviation between the engineering model and compressor geometry. The most obvious is the gap between the top and bottom halves of the stationary components that can open up when the compressor is fully pressurized. Again, steps can be taken to seal this split gap (i.e., split gap o-ring or other sealants) but if it is not properly done or if the gap is larger than expected, additional leakage between stages can occur, resulting in differences between predictions and test results. Another potential source of discrepancy is the method used to split the two halves of the stationary components. For example, if the parts are saw cut, the width of the saw blade or the amount of material removed by the saw cut can be of concern, especially in very small compressors. This is especially true when the cut is through diffuser or return channel vanes. This can lead to a misalignment of the vane surface between the top and bottom half. The impact in most cases would be very small but it could become an issue if vane is cut at an acute angle (see Figure 16).

Figure 15 – Rotor being installed in bottom half of a horizontally-split compressor

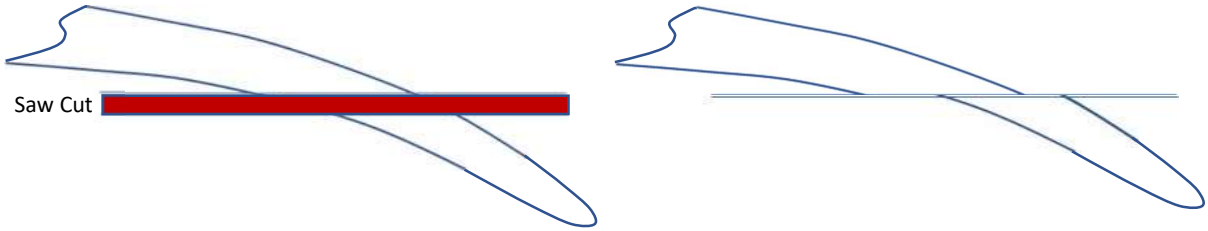

Figure 16 – Impact of saw cut on stationary vane alignment (*exaggerated*)

Before moving away from the subject of manufacturing, please note that there are many more publications available in the open literature that address the impact of manufacturing accuracy on compressor performance including Childs & Noronha (1997), Cousins et al (2014), Cave & Ji (2017), Peng et al (2017) and Frier et al (2020). Those interested in more detail in this area are encouraged to obtain copies of those papers as well as the references cited in those works.

TEST UNCERTAINTIES

Despite recent advances in computational fluid dynamics (CFD) and other sophisticated analytical methods, testing continues to play a vital role in the development of high-performance centrifugal compressor stages. Moreover, the factory acceptance test (FAT) and/or the field acceptance test serve as the final proof that the compressor meets the predicted design and contractual performance.

Performance testing can also be used as part of a new aerodynamic stage component design process, to confirm the results predicted by the analytical design methods. Additionally, it could be used for troubleshooting purposes, to identify the reasons for which a certain machine, or one of its components is not performing as expected. Most OEMs rely on single or multi-stage test vehicles to validate the performance of new components or stages, especially when said components or stages represent a significant departure from prior experience. (see Sorokes & Koch, 1996 and Sorokes et al, 2009, Sorokes et al, 2017, Sorokes and Welch, 1991, Sorokes and Welch, 1992, Benvenuti, 1978; Kotliar et al, 1999).

Compressor manufacturers are faced with demands for ever-increasing levels of efficiency and flow range while at the same time being asked to keep development costs to a minimum. At times, schedules do not permit the use of test rigs and designers must resort to gathering validation data from production equipment. Consequently, engineers have found it necessary to apply more complex instrumentation in environments that appear harsh when compared to the pristine nature of a single stage test vehicle in a development laboratory. Still, the data is critical to confirm the viability of new designs as well as to calibrate or validate the analytical methods used to design the new components and predict their performance characteristics.

Typically, measurements on the manufacturer's production test stand or in the field, are limited to instrumentation installed at the compressor inlet and discharge flanges [ASME, 1997] as shown at the left in Figure 17. Such probes typically measure: a) inlet pressure (static and total); b) inlet total temperature; c) inlet mass flow; d) discharge total pressure; and e) discharge total temperature. In the case of a single stage compressor, this may be sufficient to understand the performance of that stage. However, in a multi-stage compressor, instrumentation at the main inlet and main discharge is inadequate to obtain sufficient data to understand the performance characteristics of the individual stages.

In a quest for more detailed information, some manufacturers will install instrumentation at various locations within the compressor to gather so-called "stage data" [Sorokes & Koch, 1996, Borer et al, 1997]. Typical locations for this instrumentation are shown at the right in Figure 17. These instruments usually consist of Kiel-head total pressure probes, static pressure taps, and half-shielded or shielded thermocouples. In some instances, pressure or temperature rakes may be employed to measure the pressure or temperature distribution across the flow passage. All of this information can be very important in discerning the performance of the stages. However, if the probes are not properly aligned with the gas flow, the accuracy of the measurements may be compromised.

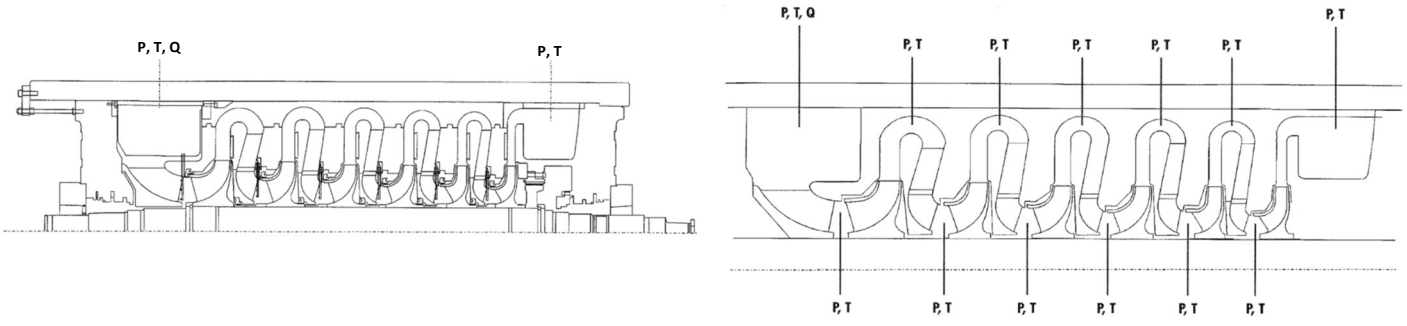

Figure 17: Cross-sections showing typical locations for instrumentation placement for flange to flange (left) and stage data (right).

Typical Kiel-head probes (Figure 18) have a range of insensitivity to incidence angle of ± 25°. If the gas is approaching the probe at an angle greater than ± 25° with respect to the probe centerline, the accuracy of the total pressure measurement will deteriorate. This limitation was normally overcome in the laboratory rig via traverse based multi-hole probes, which could be rotated automatically or manually to align the probe with the approaching flow [Dieter, 2002, Smout & Ivey, 1997, Roduner et al, 1998]. However, such probes are not practical in a production multistage compressor environment. An attractive alternative to the traverse-based system is the multi-hole probe (Figure 19) used in a non-nulling configuration and installed at a fixed position [Gilarranz et al, 2005, Sorokes et al, 2009]. When properly installed and calibrated, multi-hole probes, and more specifically 5-hole probes, can acquire very accurate pressure measurements. More importantly, these probes will provide the flow angle and velocity of the gas, which makes them very attractive for development testing of new, high performance centrifugal stages.

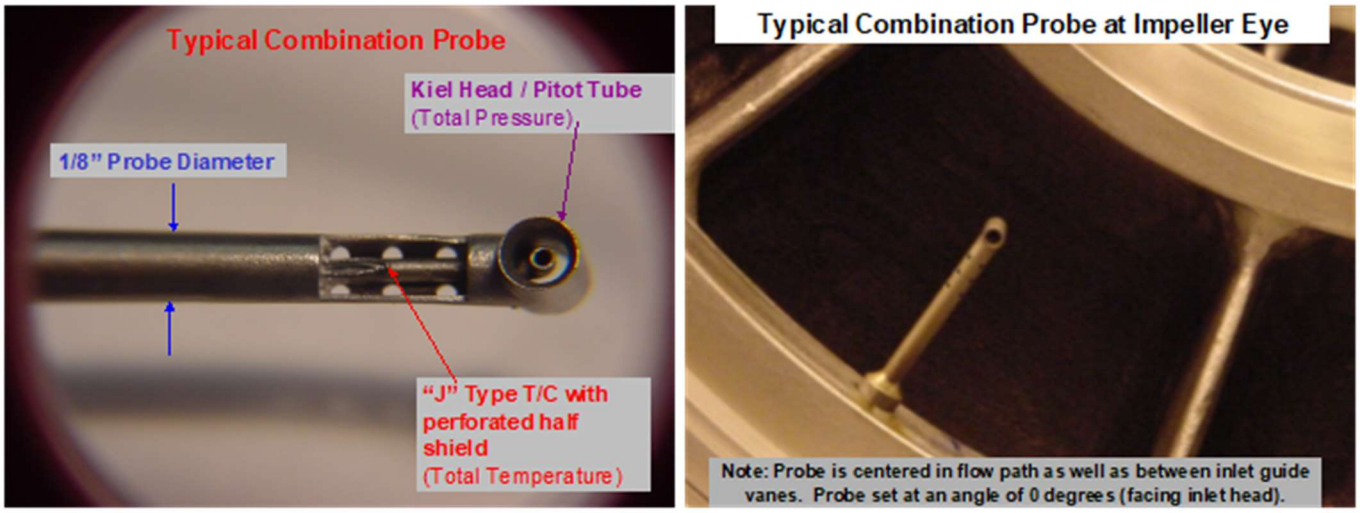

Figure 18: Combination Total Pressure/Total Temperature Probe. Probe tip detail (left), example of a probe located at the exit of an inlet guide vane - IGV (right).

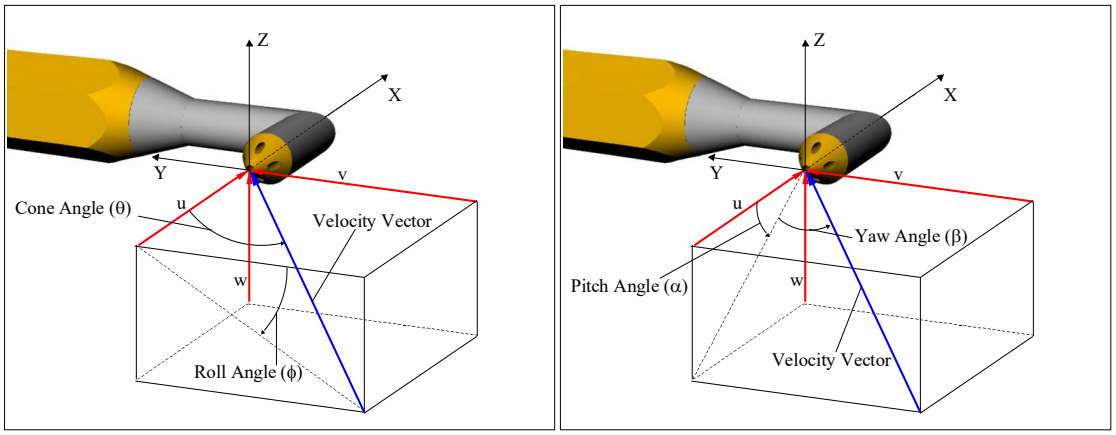

Figure 19: 5-hole Probe coordinate system and angle conventions.

In addition to accurate pressure and flow angle measurements, the performance evaluation of a centrifugal compressor stage also requires accurate temperature measurements. When the compressor is handling an inert gas during a factory acceptance test, the total temperature is typically measured using thermocouples or RTDs with the temperature probe directly in contact with the test gas, which provides faster response time and more accurate measurements. RTDs are typically more accurate than thermocouples but thermocouples are generally more robust and are preferred for testing in industrial test facilities when the sensing element is exposed to the gas.

The total temperature of the gas might be measured using half-shielded type temperature probes, as the one seen in Figure 18. These are widely used for turbomachinery measurements. Alternatively, a Kiel type shroud may be used on total temperature probes to reduce their sensitivity to flow angularity. There are several references that contain details design suggestions for this type of probes [Eckardt, 1986, Smout, 1996, Saravanamutto, 1990, ASME, 1979]. For the case of measurements at the inlet and discharge flanges, both of the above-mentioned probes are adequate, nevertheless, the lower cost of half-shielded thermocouples makes them more attractive.

When factory tests involve hazardous gases, the temperature measurements are usually performed utilizing RTDs mounted in thermowells that are inserted/welded into the piping to avoid leakage of the process gas. This leads to less accurate temperature measurements, which will directly impact the agreement between prediction and test.

Several measurement devices can be used to quantify the flowrate handled by the compressor. Some examples are: orifice plates; pressure-balanced, multi-hole orifice plates; venturi flowmeters, V-cone flowmeter, etc. The degree of accuracy of these devices will be a function of the how they are installed and where they are located within the test loop, whether they are calibrated, and if so, the range of conditions over which they were calibrated. The single orifice plate is widely used for FATs due to the simplicity of its design and the relatively low cost. However, in some cases, other methods may be selected when special requirements on accuracy and/or restrictions on the pipe size and arrangement does not allow the long length of straight piping required upstream and downstream of the measurement element. For machines in the field, the preference is to use measurement elements that do not have a significant permanent pressure drop (i.e., venturi type flowmeters).

Factory Testing of Centrifugal Compressors

Since centrifugal compressor acceptance tests are the only reliable method available to verify that the compressor will perform as required in the field, it is important that the results of such test programs accurately represent the real behavior of the machine. Although most tests confirm that the machines are performing as expected, identifying performance shortfalls during acceptance tests, i.e., while the machines are still at the manufacturer's facility, will save both the OEM and client significant time and money.

As suggested above, the accuracy of the test results is critical. Therefore, the quality of the measurements will have a direct impact on the accuracy of the results. One way to verify the quality of the measurements and associated data is to perform an uncertainty analysis. This analysis permits the evaluation of the accuracy and usefulness of the data and provides confidence that the data represents the machine's true behavior. Another use of the uncertainty analysis is to predict the accuracy that can be achieved with the instrumentation selected when planning the test. This permits one to determine if the selected instrumentation will provide a low enough level of uncertainty such that the test accuracy goals are met.

The remainder of this section presents thoughts related to the use of an uncertainty analysis to estimate the errors in data obtained during factory aero-performance acceptance tests of centrifugal compressors.

The most widely accepted test code for the aero-performance evaluation of centrifugal compressors is the ASME PTC-10 (Performance Test Code for Compressors and Exhausters) [ASME, 1997]. This code, in combination with other supporting ASME codes, is used worldwide among compressor manufacturers as well as end users. Other codes available for the evaluation of compressor aero-performance are VDI 2045 [Verein Deutscher Ingenieure, 1993] and ISO 5389 (1992). In general, these codes describe the procedures and requirements that must be met during the planning, setup, execution and evaluation of compressor aero-performance tests.

The ASME PTC-10 code allows two types of tests, Type 1 and Type 2 respectively, which are conducted under operating conditions (machine speed, gas flowrate and inlet pressure and temperature) which guarantee that the tests conditions are aerodynamically similar to those encountered in the field. A Type 1 test must be conducted on the specified gas and allows very small deviations between the test and the expected operating conditions. A Type 2 test is conducted with an alternate gas (typically an inert gas) and allows larger deviations between the test and field conditions. For both types of tests, it is important that the volume reduction is the same for both the test and the specified design condition. In addition, the Reynolds number (Re) and Machine Mach number (U_2/A_o) must be kept close to the values at the expected design conditions.

Type 2 aero-performance tests performed by the OEM typically include the measurement of seven test points to determine the machine performance at seven different operating conditions. Five of these points are measured at the prescribed test design speed and evaluate the machine performance over the full operating range at that particular speed. Two additional points are taken close to the surge condition at off-design speeds, i.e., 105 and 90% of the test speed. These points are used to establish the slope of the surge line.

As discussed in the work of Colby [2005], the OEM needs to pay special attention when selecting the type of gas and conditions at which they will conduct the factory acceptance test. The ASME test code provides guidance on the allowable variations that are acceptable for several key parameters to ensure that similitude is maintained between the test and field conditions.

It is important that the volume reduction between the stages during the test is similar (within a certain margin) to the volume reduction in the field. It is typically not possible to perfectly match the test and field volume reduction of each stage. Nevertheless, efforts should be made to adjust the inlet pressure, gas composition and test speed to provide the best balance through the stages [Colby, 2005]. The client or end user should request a plot of the test curve overlayed on the specified curve from the OEM to ensure that the test conditions meet the objectives of the test program.

The machine Mach number is also an important parameter that must be maintained. As shown in ASME, 1997, as the expected machine Mach number in the field increases, the allowable tolerance margin between the test and the field for this parameter reduces, meaning

that the test conditions need to be selected to ensure that the machine Mach number expected on test is sufficiently close to the value expected in the field.

When selecting the inlet pressure level for the test, special consideration must be given to the available power of the test stand driver, the Reynolds number that will result, and the heat loss through the compressor casing. The inlet density is directly related to the inlet pressure, and as the inlet pressure increases, a larger mass flow will be required by the machine to maintain the required volumetric flowrate. The mass flow will impact the power consumption of the machine during the test, so special care must be taken to ensure that the shop driver has sufficient power.

The Reynolds number relates to the boundary layer and frictional losses acting on the gas as it passes through the flow path. Type 2 testing is almost always conducted at a lower Reynolds number as compared to field conditions. This results in higher frictional losses, lower head and lower efficiency levels than what would be expected in the field. The ASME test code [ASME, 1997] provides guidance on the allowable departure in test Reynolds number relative to the design value, as well as the correction factors that could be applied to the test results to account for Reynolds number effects. The correction factor is not linear, the lower the absolute Reynolds number, the higher the correction factor. Since many end-users do not allow the OEM to correct the test data to account for the differences in the Reynolds number, the OEMs have to carefully set the test conditions and inlet pressure at a level that can be handled by the shop driver while also staying close to the specified Reynolds number. This minimizes the negative effects that the lower Re number can have on the test results.

Measured Quantities (Test Primary Variables):

A schematic of a typical closed loop test circuit utilized for performance testing centrifugal compressors is shown in Figure 20. The total pressure and total temperature are measured at the inlet and discharge of the machine. These measurements are used in combination with the gas properties to define the thermodynamic states at these locations.

The flowrate is measured via an adequate flowmeter. Typically, an orifice type flowmeter is utilized. However, a venturi or nozzle type flowmeter may also be used. For industrial type test facilities, it can be costly to keep an available library of venturi or nozzle type flowmeters to cover every possible combination of test loop pipe sizing and associated mass flow range. Conversely, orifice type flowmeters are easy to design and relatively inexpensive to manufacture, while offering acceptable accuracy if installed and used correctly [ASME, 1971]. The mass flow is calculated by measuring the static temperature and pressure upstream of the measurement device and the pressure drop across the element, and utilizing expressions derived for the selected type of flowmeter [ASME, 1971]. The selection of the appropriate expressions and associated coefficients is based on the type (location) of the pressure measurements (i.e., flange taps, vena contracta taps or 1D and 1/2D taps) as well as some geometric dimensions of the pipe and orifice element (pipe inner diameter and orifice diameter). The thermal expansion coefficient for the restriction element is also used for the mass flow calculations.

In addition to the above-mentioned variables, the machine rotating speed, the driver power (if available) and the diameter of the compressor impellers, are also used in the calculation of some performance parameters.

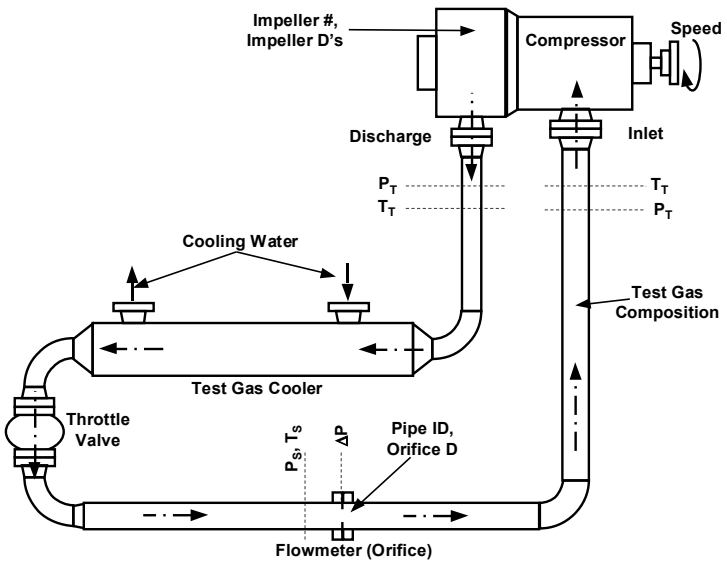

Figure 20: Schematic of a closed-loop test rig. Adapted from ASME PTC-10 [ASME, 1997].

After the above-mentioned parameters are measured, the thermodynamic states and associated conditions are calculated at the inlet and discharge as well as upstream of the flowmeter element. This is done via real gas equations of state, which adequately represent the behavior of the test gas [Grosso, 2020]. The use of real gas equations of state is particularly important for Type 1 and in-situ field performance tests. For the uncertainty analysis method discussed herein, this is accomplished by the use of a third-party thermodynamic property calculation package (Design II from WinSim), which permits the use of several real gas equations of state (Sandberg, 2005).

The measured and calculated thermodynamic data is then used to calculate the relevant parameters, shown below, which are used for the compressor performance evaluation [Schultz, 1962, ASME, 1997, ASME, 1971, and Grosso, 2020]. The description of the variables and the units of measurement used in these equations are included in the nomenclature section at the end of the paper. The complete set of equations used for performance evaluation may be found in reference [ASME, 1997, Gilarranz, 2005, Gilarranz, 2006].

- Polytropic and isentropic Exponents (n, n_s)

$$n = \frac{\ln\left(P_2/P_1\right)}{\ln\left(V_1/V_2\right)} \qquad n_s = \frac{\ln\left(P_2/P_1\right)}{\ln\left(V_1/V_3\right)} \tag{2,3}$$

- Polytropic Work or Head (Wp)

$$W_p = f\left(\frac{n}{n-1}\right) \quad (P_2V_2 - P_1V_1)\ 144 \tag{4}$$

- Gas Power (P_G)

$$P_G = \frac{WF\ \ (H_2 - H_1)}{42.408} \tag{5}$$

- Weight Flow (WF) (Equation for an Orifice Plate)

$$WF = 31.501\ K\ Y_o\ d^2\ Fa\ \sqrt{\rho_{ori}\,\Delta P_{ori}} \tag{6}$$

- Volume to Speed Ratio (Q/N)

$$\frac{Q}{N} = \frac{WF\ V_1}{RPM} \tag{7}$$

- Flow Coefficient (ϕ)

$$\phi = \frac{WF}{\rho_1\ 2\pi\ RPM\left(\frac{DIA_1}{12}\right)^3} \tag{8}$$

- Polytropic Efficiency (η_p)

$$\eta_p = \frac{W_p}{(H_2 - H_1)\ \ 778.16} \tag{9}$$

- Polytropic Work Coefficient (μ_p)

$$\mu_p = \frac{32.174\ \ W_p}{\sum\left(\frac{\pi\ \ \text{Dia.}\ \ \text{RPM}}{720}\right)^2} = \frac{32.174\ \ W_p}{\left(\frac{\pi\ RPM}{720}\right)^2\left(\sum\left(Dia^2\right)\right)} \tag{10}$$

- Work Input Coefficient (W_{in})

$$W_{in} = \frac{32.174\ \ (H_2 - H_1)\ 778.17}{\sum\left(\frac{\pi\ \ \text{Dia}\ \ \text{RPM}}{720}\right)^2} = \frac{32.174\ \ (H_2 - H_1)778.17}{\left(\frac{\pi\ RPM}{720}\right)^2\left(\sum\left(Dia^2\right)\right)} \tag{11}$$

The equation for the weight flow is based on the expressions included in the ASME PTC 19.5 test code [ASME, 1971] for the case of orifice type flowmeters. Alternate expressions are available for other flow measurement devices

The last five parameters are generally used to graphically depict the compressor performance. The polytropic efficiency (η_p), head coefficient (μ_p), and work input coefficient (W_{in}) are plotted as a function of the flow coefficient Q/N and/or ϕ. A sample plot showing the predicted curves (solid lines) compared with the experimental data points (dashed line) is shown in Figure 21.

Some performance test codes [Verein Deutscher Ingenieure, 1993, ISO, 1992] recommend that the test data is plotted with the associated uncertainty in the measurement. This is done by plotting an ellipse around each test point. The semi-axis of the ellipses are proportionally sized to the uncertainty in the measurement of the flow coefficient (horizontal semi-axis) and the values of efficiency, head coefficient and work input coefficient (vertical semi-axis of each respective ellipse). A sample of this approach is also shown in Figure 21 (the ellipses have been enlarged to help the reader to visualize the concept).

Once the test is complete, the as-tested performance data is used to modify (or calibrate) the analytical model that represents the performance of the machine, in order to generate the as-tested compressor operating maps for the site operating conditions to allow the OEM and end user to determine if the contractual obligations have been met within the agreed upon limits. As mentioned previously, the commercial implications associated with the use of acceptance test data require the test uncertainty levels be considerably lower than the acceptance test tolerance margins. There are several methods that can be utilized to estimate the uncertainty of the test data [Verein Deutscher Ingenieure, 1993, ASME, 1998, ISO, 1993]. The next sections will present the results of an analysis to estimate the uncertainty levels of the test data obtained from a Type 2 performance test. This approach may also be extended to Type 1 and in-situ field performance tests.

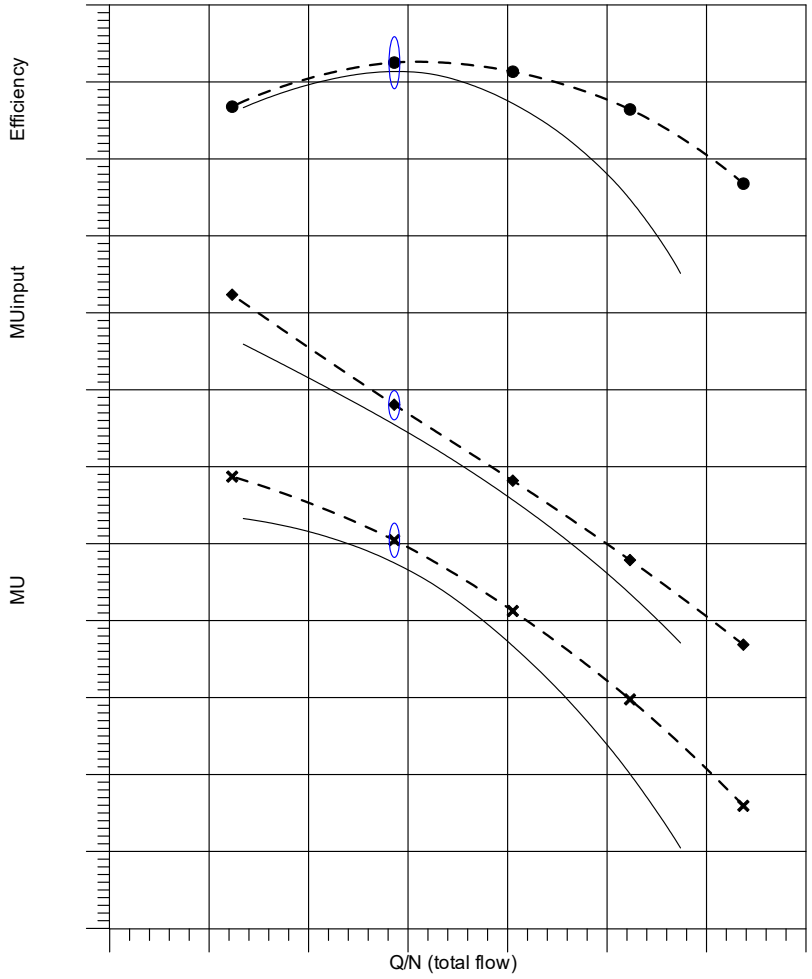

Figure 21. Typical Non-dimensional performance curves with uncertainty ellipse surrounding the test point corresponding to the design condition

Uncertainty Analysis

Every measurement has an associated level of error, which results from the difference between the measured value and the true value of the parameter that is being measured. As shown in Figure 22, this difference is defined as the total error (δ) and results from the

combination of a random component (ε) and a systematic component (β). Unfortunately, the true value of the parameter being measured is unknown, hence the magnitude of the measurement error cannot be directly calculated and must be estimated.

Several authors have published work concerning methods to estimate the uncertainty of experimentally measured data and the associated parameters that can be derived or calculated from the measurements [Kline & McClintock, 1953, Moffat, 1982, Coleman & Steele, 1998, Gilarranz, 2005, 2006]. These references present an extensive description of the systematic and random error components, as well as methods to estimate their magnitude and to combine their effects into an overall uncertainty value that can be used with a certain confidence level (typically 95%). The sources that introduce uncertainty in a measurement system may be divided into the following categories [ASME, 1998]:

- Calibration Uncertainty
- Data Acquisition Uncertainty
- Data Reduction Uncertainty
- Uncertainty due to Methods
- Other Sources

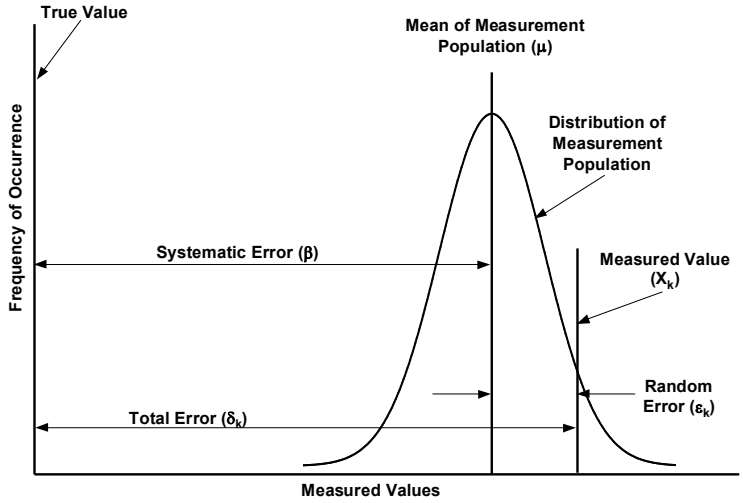

Figure 22: Illustration of the components of the measurement errors. Adapted from ASME PTC 19.1 [ASME, 1998].

The work discussed herein is intended to help visualize the effects of measurement uncertainty over the parameters that are usually used to evaluate the compressor performance. It is based on studies previously published by the OEM [Gilarranz, 2005, 2006] related to the uncertainty analysis developed to estimate the error levels in data gathered during factory acceptance tests of single- or multi-stage centrifugal compressors. The method utilizes the polytropic compression model and equations for compressor performance evaluation included in the ASME PTC-10 test code [ASME, 1997]. The analysis incorporates the effects of the variation and uncertainty levels associated with every parameter used to calculate compressor aero-thermal performance. Included are the variables used to define the thermodynamic states of the fluid inside the compressor, as well as geometric and operational parameters associated with the machine and test loop. In addition, real gas equations of state were incorporated into the calculations to avoid errors associated with inadequate estimations of the gas thermodynamic properties. Though of limited importance for some test gases, some applications require test gases that significantly deviate from the ideal gas approximations.

The following list contains the primary variables used for the evaluation of the compressor aero-performance. These variables are measured before or during the test and are used to derive and/or calculate the other parameters that are relevant for compressor performance evaluations [Gilarranz, 2005, 2006]. The effect of some of these primary variables on machine performance is small. Nevertheless, they were included in the study to assess their level of contribution and to verify that indeed their effect is negligible.

Primary Variables: T_1, P_1, T_2, P_2, T_{ori}, P_{ori}, ΔP_{ori}, RPM, D, d, Fa, DIA, DIA_1

The first step taken for the uncertainty analysis was to determine the methods to estimate the random (or precision) and the systematic (or Bias) components of the uncertainty associated with the measurement of these primary variables. References [ASME, 1998] and [Coleman & Steele, 1998] provide a detailed description of the expressions and methods used for this purpose.

The total uncertainty interval for 95% confidence level (U_{95}) can be calculated by [ASME, 1998]:

$$U_{95} = 2\sqrt{\left(\frac{B}{2}\right)^2 + (S_{XM})^2} \tag{12}$$

In this expression, B is the combined effect of all systematic uncertainty sources and S_{XM} is the random uncertainty contribution. The true measured value (x) is then assumed (with a 95% confidence level) to be contained within the following interval of the measured value (X_M):

$$X_M \pm U_{95} \tag{13}$$

The uncertainty of the remaining parameters used for performance evaluation, which are derived from the primary variables, was estimated by propagating the primary variables uncertainties through the respective expressions used in the calculation of the performance parameters.

Once the random and systematic components were established for each variable, the total uncertainty associated to said variable was estimated by the following equation [ASME, 1998]:

$$U_{R95} = 2\sqrt{\left(\frac{B_R}{2}\right)^2 + (S_R)^2} \tag{14}$$

In this expression, B_R corresponds to the combined effect of all systematic uncertainty sources affecting the result and S_R corresponds to the random uncertainty contribution. The true resultant (R) is then assumed (with a 95% confidence level) to be within the interval:

$$R_M \pm U_{R95} \tag{15}$$

It is important to state that the random contribution to the measurement error can be reduced by averaging multiple measurements and using averages instead of the individual measurements for the calculation of the derived parameters. The systematic error components of measurements can be reduced by proper selection, calibration and installation of the instruments being utilized as well as by adequate design of the data acquisition and data reduction processes.

Sensitivity Coefficient Approach

Most performance parameters are not measured directly but rather derived based on the measurement of basic parameters, which are then combined using a mathematical expression which represents the given parameter as a function of the primary variables. The uncertainty levels of these results are estimated by propagating the uncertainties associated to the primary variables through the calculations. This is done by calculating the so-called sensitivity coefficients, which correspond to the ratio of the change in the result due to a unit change in the value of one of its measured parameters. These sensitivity coefficients can be calculated either analytically or numerically. The analytical approach is used when there is a mathematical relationship (G) between the result and the measured parameters. The sensitivity coefficient (θ_i) of the parameter (g_i) is obtained by partial differentiation of the mathematical expression with respect to that particular parameter (g_i).

$$\theta_i = \frac{\partial G}{\partial g_i} \tag{16}$$

The numerical approach is required when a closed form expression is not readily available for G. For this case, a perturbation analysis is performed and finite increments in the value of a parameter are used to evaluate the changes in the result due to the perturbation. The sensitivity coefficients are then calculated as:

$$\theta_i = \frac{\Delta G}{\Delta g_i} \tag{17}$$

The random uncertainty component of a result is estimated by using the following expression [ASME, 1998]:

$$S_R = \left[\sum_{i=1}^{j} (\theta_i S_i)^2\right]^{1/2} \tag{18}$$

where, S_i is the standard deviation of the mean of the measured parameter g_i.

Similarly, the systematic uncertainty component of a result is estimated by using the following expression [Coleman & Steele, 1998]:

$$B_R = \left[\sum_{i=1}^{j} (\theta_i B_i)^2 + 2\sum_{i=1}^{j-1}\sum_{k=i+1}^{j} \theta_i \theta_k B_{ik}\right]^{1/2} \tag{19}$$

B_i is the systematic uncertainty of the measured parameter g_i, while B_{ik} represents the correlated systematic uncertainty, which results when one or more of the primary variables share systematic uncertainty sources. Since the value of B_{ik} must be approximated, initially

it was assumed that the primary variables did not share any sources of systematic uncertainty and/or the contribution of these sources was negligible. Therefore, the second term in the above equation was not initially considered [Gilarranz, 2005]. Further investigations were carried out to establish appropriate ways to estimate and/or quantify the correlated systematic uncertainty for this application. A review of this data is presented and discussed in a following section of this document and shows the impact of the correlated bias errors over the uncertainty estimation of the test data Gilarranz (2006). Note in Equation 19, that if the sensitivity coefficients θ_i and θ_k are of different signs (i.e., one is negative and one is positive), then the effect of the correlated bias is to reduce the overall value of the uncertainty for that parameter. If the signs are the same, the correlated bias will increase the levels of uncertainty.

Another important aspect to highlight is that the use of a perturbation analysis for the calculation of the sensitivity coefficients allows the uncertainty analysis to be easily adapted into a spreadsheet that can be populated using data created for this purpose using the data reduction subroutines and calculations that are available within the data acquisition program used by the OEM at their test stand. This can be achieved by perturbing the primary variables around their nominal values and calculating the thermodynamic properties and evaluating the performance parameters at these perturbed conditions. Knowledge of the values of all parameters (thermodynamic and performance) at the perturbed and nominal conditions of the primary variables allows the calculation of the partial derivatives required for the sensitivity coefficients by numerical derivation.

***Measurements and Accuracy*:**

This section presents the techniques typically employed for the measurement and/or quantification of the primary variables measured before or during the performance tests. These techniques correspond to the best practices recommended in the current version of the international standards that are applicable to the measurement of each particular parameter.

The exit diameter of each impeller is measured with external micrometers or a CMM before the rotor is installed in the compressor. This provides the test engineer with the geometric data used for the flange-to-flange performance calculations, i.e., first impeller diameter (DIA_1) and machine equivalent diameter (DIA).

The inside pipe diameter and the diameter of the flow element (usually an orifice plate) are also measured using internal micrometers. PTC 19.5 [ASME, 1971] provides guidelines concerning where the measurement must be performed and the allowable deviation between the measurements. The code also specifies the amount of straight pipe required upstream and downstream of the orifice. The orifice thermal expansion area factor (Fa) is calculated based on the static temperature of the gas upstream of the orifice [ASME, 1971]. This temperature is measured via two or four thermocouples (or RTDs) placed upstream of the orifice. The static and differential pressures are measured via static taps upstream and downstream of the orifice plate [ASME, 1971, ASME, 1987].

The machine speed is usually measured with a Keyphasor® mounted on the shaft.

As noted previously, for Type 2 tests, the total temperature is typically measured using thermocouples or RTDs with the temperature probe directly in contact with the test gas. In practice, thermocouples can be calibrated to reduce the uncertainty level to values between ±0.1 to ±0.2 F. Typically, four of these probes (circumferentially distributed) are inserted at each measurement station (i.e., inlet and discharge of the machine), following the recommendations included in the ASME PTC-10 [ASME, 1997]. For the case of low temperature ratio machines (e.g., low pressure ratio) machines, the number of probes might be increased to eight. References [ASME, 1997] and [ASME, 1979] include additional guidelines and recommendations regarding the design, installation requirement and analysis of the temperature measurements.

Total pressures are typically measured using Kiel type total pressure probes inserted into the flow passage. Typically, four of these probes are inserted into the flow at each measurement station (i.e., inlet and discharge of the compressor) following the recommendations included in reference [ASME, 1997].

For the case of flange-to-flange measurements, it is also possible to combine the capability of measuring the total pressure and total temperature into one instrument. For this, the so-called combination probes, combining a Kiel type pressure probe with a half-shielded thermocouple, can be inserted into the pipe upstream and downstream of the compressor. Since the immersion length of the probe into the flow path is larger than the one required for an interstage measurement, the probe must include a more robust design (see Figure 23). The use of these probes has the advantage of decreasing the amount of instrumentation ports that must be provided for the tests, which have to be drilled through the test loop piping.

Another parameter that must be evaluated during the tests is the test gas composition. For Type 2 tests, the most commonly utilized gases are Nitrogen, Carbon Dioxide, R134A, Helium or a mixture of these gases. For tests run with pure gases, it is fairly easy to know the gas composition. On the other hand, for tests run with gas mixtures, it is necessary to continuously monitor the gas composition to verify that the mixture remains constant during the test. This is usually done with a gravitometer, which compares the specific gravity of the test gas with that of air. The type of gas that is utilized for the test often determines the equation of state that should be used to calculate the thermodynamic properties. The use of an inappropriate equation of state for the test conditions can produce misleading

results. The use of the Design II gas property package for the work presented herein permitted the selection of adequate real gas equations of state that properly modeled the test gas behavior.

Figure 23: Combination total pressure/total temperature probe used for flange-to-flange measurements.

Data acquisition of temperature signals from thermocouples and RTDs are often made via high-accuracy multiple-channel temperature scanners. The signals from the pressure probes and/or static taps are transformed into a voltage or an engineering unit output by means of pressure transducers. The accuracy of these transducers is most times determined as a fixed percentage of their full-scale range; hence it is very important to set transducer range correctly. In general, these should be selected, so that the pressure falls within the upper 75% of the range. Multi-channel pressure scanners (pressure blocks) offer the possibility to measure several pressure signals with independent pressure transducers, which are controlled by the same electronics and are packaged within the same enclosure. The selection of the optimal combination of temperature and pressure scanners/transmitters will depend on the test facility requirements, which vary from test to test. Saravanamutto (1990) presents a detailed description of the sources of uncertainty (systematic and precision) that are characteristic of the systems that are typically used for the measurement of pressure and temperature.

All of the instrumentation used during the test should be calibrated at regular intervals. In addition, the calibration of the instrument should be checked before and after each test to ensure that the instrumentation is always in good operating condition. The calibrations that are performed at the equipment manufacturer's facility will usually be limited to the verification that the instrument is operating within the standard accuracy ranges that are quoted in the specifications. On some occasions, these levels of accuracy are insufficient to achieve the levels of accuracy required for a test. Higher levels of accuracy may be obtained by calibrating the instruments against a higher accuracy standard, and generating calibration curves that can be used during the test

Assumptions and Considerations

The uncertainty analysis process presented previously corresponds to an ASME PTC-10 Type 2 performance tests, following the recommendations set forth in references [ASME, 1997, ASME, 1971, ASME, 1998, ASME, 1987 and ASME, 1979]. The following considerations must be considered when using this method for the reduction of performance data from centrifugal compressor tests obtained following other procedures and/or standards.

The flow at the locations where the pressure and temperature are measured is assumed to be fully developed, uniform and with a negligible swirl component. This can be achieved if the measurements are made at adequate locations and if the test loop is arranged following the recommendations set forth in reference [ASME, 1997]. High values of swirl can cause the flow to have a large incidence angle with respect to the axis of the pressure and/or temperature probes, which may result in incorrect measurements. The quality of the measurements will also be affected (deteriorated) by flows in which large velocity or temperature gradients are present in the vicinity of the measurement probe location. For this case, the measured data will not represent the average values of pressure and temperature that are present at that particular measurement station.

As a sidebar, it must be noted that non-uniform and/or swirling flow entering the compressor inlet can also have a detrimental impact on the performance of the first stage in the machine. An example of this situation was described in a case study by Aikens et al (2020). In this situation, the piping arrangement used on the production test stand was causing a non-uniform flow field at the compressor inlet, which in turn caused a reduction in the efficiency and head coefficient of the first stage impeller. The problem was initially diagnosed as a problem inside the compressor, but an RCA identified the unacceptable piping arrangement. After correcting the piping deficiency, the compressor met the guarantee requirements.

The temperature and pressure measurements at the inlet and exit of the compressor are assumed to be at total (stagnation) conditions. If the measurements are at static conditions, then the effects of the gas velocity over the measurements should be accounted for. This effect is negligible if the local Mach number at the measurement location is below 0.1.

The temperature measurements are assumed to be taken with the sensing element directly submerged in the flow field (no thermowells). If this is not the case, then the effect of the thermowell over the accuracy of the measurement should be taken into account as a systematic component of the error.

The flowrate is assumed to be measured using an orifice type flowmeter with pipe tap (radius) measurements. The orifice must be properly manufactured and installed following appropriate standards [ASME, 1971]. The extension of this work to accommodate other flowmeter types is possible as long as the appropriate changes are made to the sensitivity coefficients.

Application Example

The following paragraphs and figures represent a brief summary of the work of Gilarranz (2005 and 2006). This section is included to illustrate the effect that the uncertainty in the key measured variables may have over the uncertainty levels that can be expected for the performance parameters used to quantify the aerodynamic performance of the machine. Comments are also included to show how the correlated bias error can reduce the overall uncertainty of the results.

Figure 24 presents the contributions to the uncertainty level for the measurements of mass flow and flow coefficient (Q/N) that can be attributed to each one of the primary variables for a multistage compressor factory acceptance test. As may be seen in the figure, the major contributor is the error associated with the measurement of the pressure drop across the orifice element. As discussed later (below) this error in ΔP also contributes to about 40% of the total error associated with the measurement of the power consumed by the compressor. Therefore, special efforts should be directed towards the minimization of the error in the measurement of this variable. This may be achieved by selecting lower pressure transducer ranges (if possible) as well as by increasing the accuracy of the instrument.

Figure 25 presents the contributions to the uncertainty level for the same parameters, including the effects of the correlated bias errors in the measurement of P, T and the pipe and orifice diameters (D and d). As may be seen in the figure, all of the correlated bias error components are negative, which means that they have the effect of reducing the overall uncertainty levels of the resulting measurements.

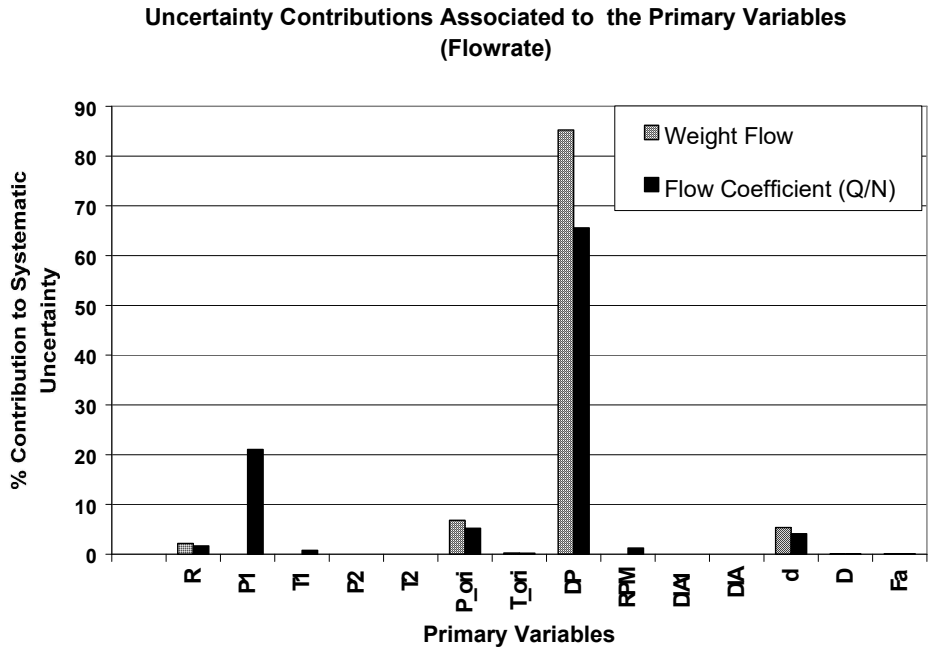

Figure 24: Contributions of the uncertainty level of each primary variable to the uncertainty in the measurement of the flow and flow coefficient (Q/N).

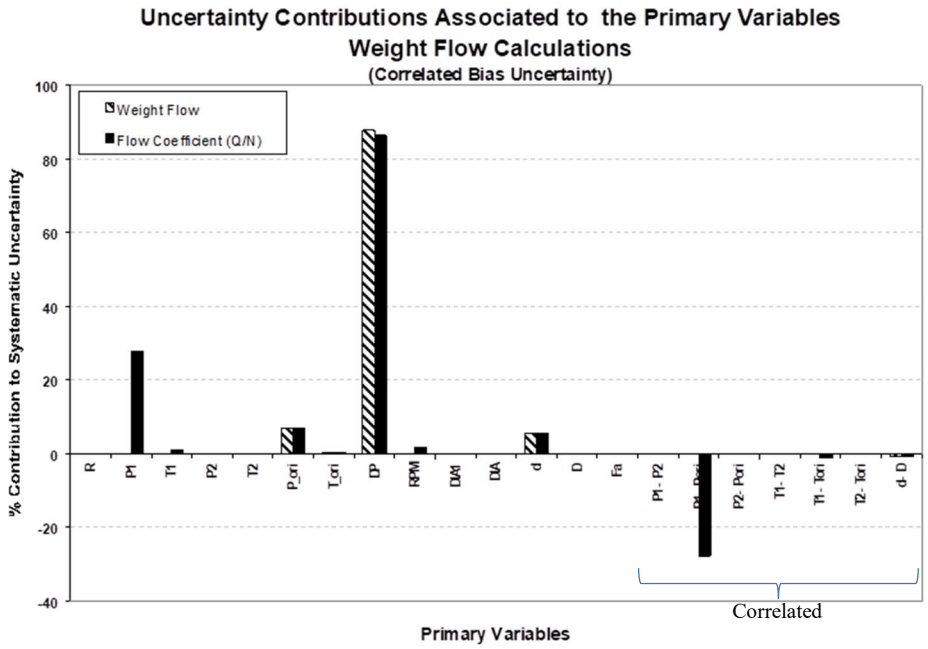

Figure 25: Contributions of the uncertainty level of each primary variable to the uncertainty in the measurement of the flow and flow coefficient (Q/N). Includes the effects of correlated bias errors.

Figure 26 presents the contributions to the uncertainty level of the measurements of the main performance parameters (Wp, PG, η_p, μ_p, W_{in}). that can be attributed to each one of the primary variables. Note that the polytropic work and the polytropic work coefficient (μp) are affected mostly by the uncertainty in P_1 and P_2. The compressor gas power is affected by the error in ΔP (40%), T_1 and T_2. The work input coefficient is affected by T_1 and T_2, and the polytropic efficiency is affected by P_1(65%), P_2, T_1 and T_2. For this case the errors in the temperature measurement were estimated to be 0.35°F, which corresponds to carefully calibrated thermocouples or RTDs.

Figure 27 presents the contributions to the uncertainty level for the same parameters, including the effects of the correlated bias errors in the measurement of P, T and the pipe and orifice diameters (D and d). This figure shows the strong effect that may be attributed to the correlated bias error components. As discussed in Figure 26, the polytropic work and the polytropic work coefficient (μ_p) are affected mostly by the uncertainty in P_1 and P_2. The compressor gas power is affected by the error in ΔP, T_1 and T_2. The work input coefficient is affected by T_1 and T_2, and the polytropic efficiency is affected by P_1, P_2, T_1 and T_2. For this case the errors in the temperature measurement were estimated to be 0.35°F, which corresponds to carefully calibrated thermocouples or RTDs. In Figure 27 the negative sign of some of the correlated bias contributions causes the total uncertainty of some parameters (term B_R or equation 19) to be considerably lower than the individual contributions (terms $(\theta_i B_i)^2$ and $\theta_i \theta_k B_{ik}$ of equation 19). This leads to the large maximum and minimum limits shown on the vertical scales of the plots.

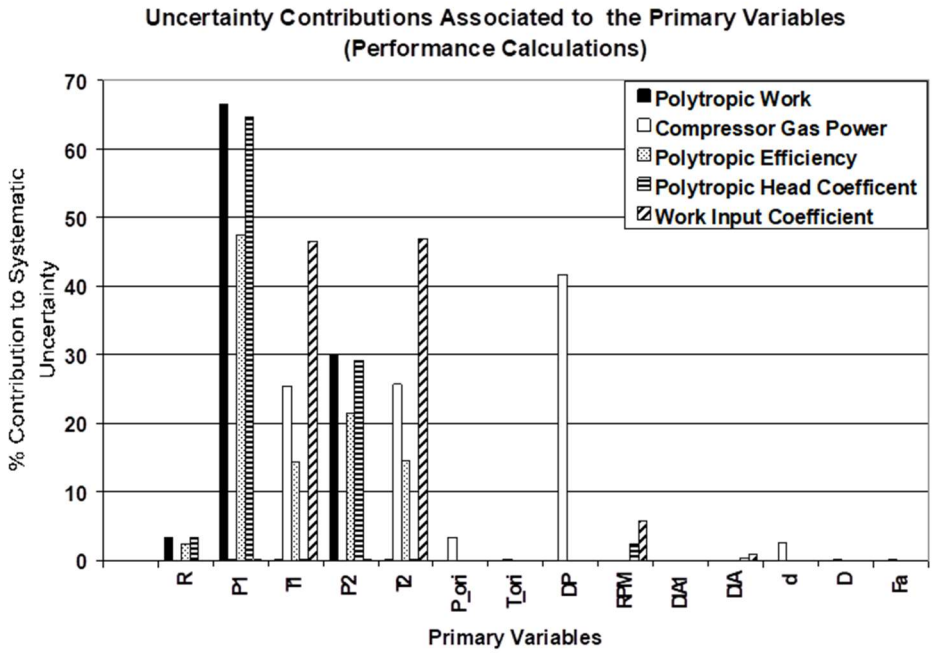

Figure 26: Contributions of each primary variable to the uncertainty in the measurement of the main performance parameters

.

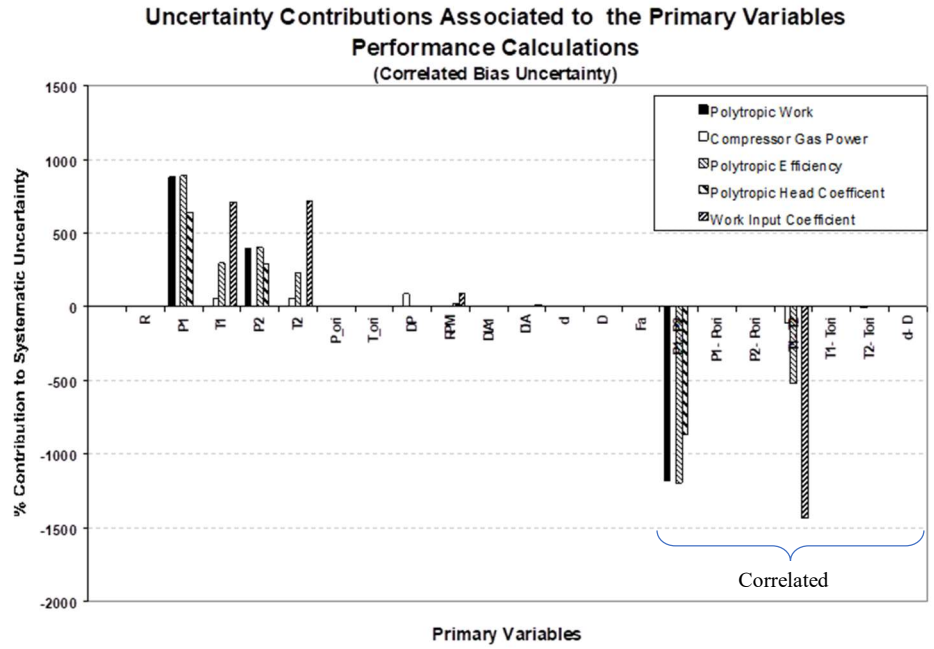

Figure 27: Contributions of each primary variable to the uncertainty in the measurement of the main performance parameters. Includes the effects of correlated bias errors

Figures 28 shows the effects of the uncertainty in the measurement of temperature (assumed to be the same for T_1 and T_2) over the uncertainty in the measurement of polytropic efficiency for tests conducted on machines with different levels of pressure ratio and tested with CO_2. Note that the results shown in the figure correspond to an increase (above the nominal value of uncertainty) that would be observed for the increasing uncertainty in temperature (i.e., the nominal value has been subtracted for all cases). As discussed in the work of Gilarranz (2005, 2006) the behavior of the uncertainty in the measurement of gas power and the work input coefficient followed the trend observed for the polytropic efficiency. It is clear from the figure that the effect of temperature uncertainty is larger for low pressure ratio machines. Note that the temperature ratio of a compressor is directly related to its pressure ratio (or the amount of work

added to the fluid to increase its pressure levels). For high pressure ratio machines, one would typically expect a high temperature ratio. Note then, that the relative effect of the individual uncertainties in the measurement of the temperature is decreased as the temperature difference between the inlet and discharge of the compressor increases (i.e., for the case of high pressure/high temperature ratio machines). The opposite of the above is also true. A similar behavior was observed in the evaluation of the effects of the uncertainty in the measurement of pressure over the uncertainty in the measurement of polytropic efficiency (not shown in this work).This suggests that special considerations are required when testing machines that have a low-pressure ratio such as the case of pipeline boosters and/or single-stage machines.

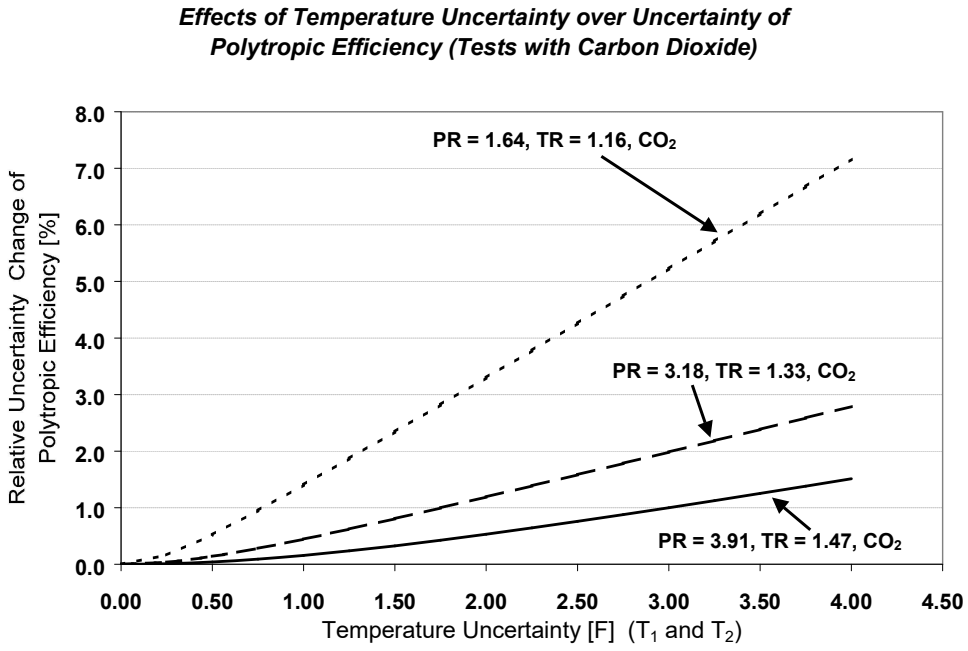

Figure 28: Effects of temperature measurement uncertainty over the uncertainty of the polytropic efficiency for operation at several pressure ratios handling CO_2 as the test gas

Figure 29 shows the effects of correlated bias errors on the relative error in the measurement of polytropic efficiency as a function of the uncertainty in the measurement of T_1 and T2 (assumed to be the same). Note that correlating the error associated to T_1 and T_2 greatly reduces the error of the efficiency.. The uncorrelated temperature errors would have to be around 0.5°F, to achieve the same levels of uncertainty as the correlated case with an error of 4°F. This means that if the temperature measurement system (thermocouples and DAQ system) is properly designed to allow the bias errors to be completely correlated, the thermocouple calibration requirements can be slightly relaxed while still assuring low levels of uncertainty in the end resulting performance parameters.

The same trends were observed when performing a study to evaluate the effect of the correlated bias associated to the measurement of the inlet and discharge pressure (P_1 and P_2). In that case it was also found that correlating the bias errors significantly reduces the uncertainty in the measurement of the performance parameters. Therefore, if the pressure measurement system (pressure scanners and DAQ system) is properly designed to allow the bias errors to be completely correlated (i.e., calibration of the equipment against the same standard), the pressure transducer calibration requirements can be slightly relaxed while still assuring low levels of uncertainty in the end resulting performance parameters.

The work referenced above also included evaluations to show the relative uncertainty of the polytropic efficiency, gas power and polytropic head coefficient as a function of the error in the measurement of T_1 and T_2, including different levels of bias error correlation. For the case of the polytropic efficiency and gas power, an increase in the level of correlation reduces the relative uncertainty of said performance parameter. On the other hand, for the case of the polytropic head coefficient, increasing the level of correlation will produce a slight increase in the relative uncertainty associated to this performance parameter. This is due to the fact that the correlated bias contribution (term $\theta_i \theta_k B_{ik}$ in equation 19) has a positive sign and hence increases the uncertainty. Even for this case, the large benefits of using the correlated systematic uncertainty for the calculation of the errors associated to the efficiency and gas power greatly outweigh the small increase that is produced in the error associated to the head coefficient.

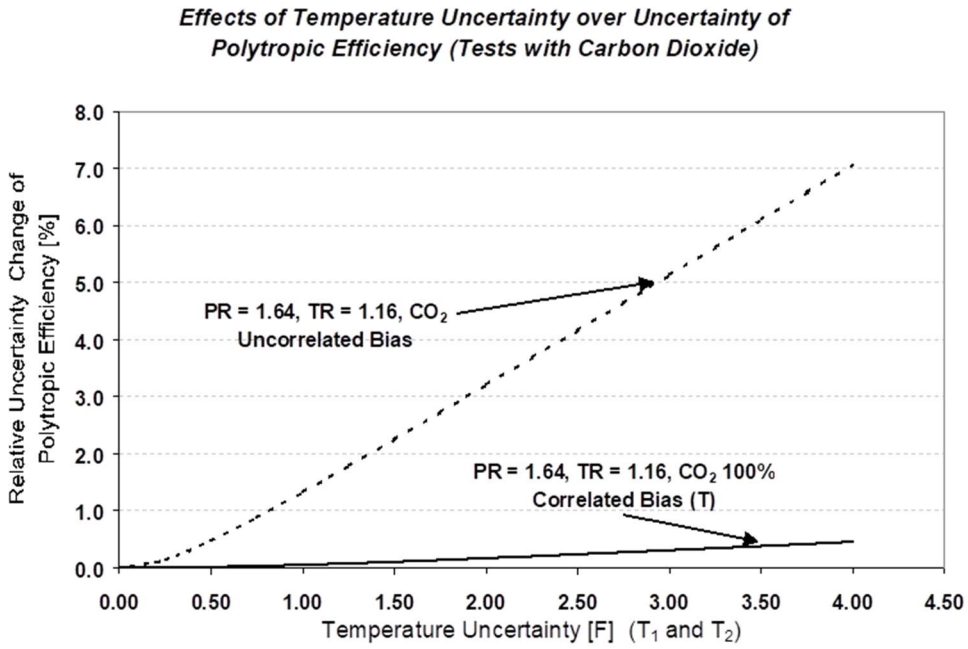

Figure 29: Effects of temperature measurement uncertainty over the uncertainty of the polytropic efficiency for operation with CO_2 as the test gas. Comparison of the results assuming correlated and uncorrelated bias errors.

Comments on Field Testing

The above comments are directed toward the evaluation of the uncertainty of test data obtained during factory acceptance tests (ASME Type 2) of centrifugal compressors. This, however, does not imply that the uncertainty analysis method cannot be applied to Type 1 tests and/or on-site field performance tests. For these cases, special considerations must be taken into account due to the fact that the test instrumentation and compressor piping setup that is available at site, is not the most adequate for testing the machines.

As mentioned above, in order to achieve accurate measurements for the evaluation of compressor performance, it is important that the instrumentation is adequately calibrated. In general, it is necessary to temporarily install special instrumentation that is used during the field performance tests. In many instances, the location within the piping that is available for the installation of additional instrumentation does not comply with the recommended practices [ASME, 1997, ASME, 1971, ASME, 1987, ASME, 1979] and hence additional levels of uncertainty must be added to the results to account for the error due to installation.

The pressure measurements performed for field tests are typically static type measurements (not total measurements), this however does not become an issue unless the local Mach number of the flow at the location of the measurement is above 0.1. Special care should be taken to ensure that the static taps are adequate for the measurement [ASME, 1987].

Many times, there is only space available for one instrument of each kind at each measuring station (i.e., one temperature probe and one pressure sensor per station). For this case, the added benefit of having multiple measurement sensors for each measured parameter is not an option, and the uncertainty associated with these measurements must be increased slightly to account for possible gradients in the flow that would not be detected by an individual measurement location.

As mentioned previously, systematic (or bias) and random errors for all of the instruments that will be used for the data collection are required for the evaluation. The random error is estimated by using the standard deviation of measurement samples for each parameter. On the other hand, the bias component will depend on the type of instrument and its respective calibration.

Thermocouples and/or RTDs are typically installed in thermowells. If the installation is old, the outer surface of the thermowells (the one exposed to the process gas) may be fouled and hence special considerations on the accuracy of the temperature measurements must be taken. The bias error for the temperature measurement devices can be obtained from the calibration data (if available) or can be estimated based on existing literature. If thermowells are used, then the Mach number of the gas at the location of the measurement must be calculated and the total temperature must be calculated based on the expressions included in ASME (1997) and ASME (1979).

Calibration data should also be available for the instrumentation and hardware used for flowmeter calculations. The flowrate plays an important factor in the calculation of the machine-required power, hence special care should be taken to obtain accurate measurements.

For the case of compressor field tests, the gas composition plays a key role in the accuracy of the calculations, therefore it is extremely important to have an accurate knowledge of the composition of the process gas that will be handled during the test. Samples should be taken for each section the same day of the test (one before the test and one after, as a minimum) and these analyses should be the ones that are used for post-processing of the test data for the final (official) performance evaluation. If a significant change in gas composition is observed between the pre- and post-test analyses, then the accuracy of the test data is probably compromised. The use of adequate real gas equations of state that properly model the behavior of the process gas is also an important factor during the test. The use of inadequate equations of state may produce results that are misleading.

The work of Gilarranz (2006) contains a sample case from field data to illustrate the effect that the gas composition can have on the apparent performance of a centrifugal compressor. The evaluation corresponded to data obtained during a field test in which the gas composition handled by the machine varied due to process disruptions in the system caused by gas field production operations. Reducing the test data using the gas composition with the lowest and the highest molecular weight can lead to different results If a lower molecular weight gas is used to reduce the data from the test, then the performance of the machine seems to improve. On the other hand, if a gas with a higher molecular weight is used to reduce the same data, then the performance of the machine seems to deteriorate. Note that for this exercise, the pressure and temperature ratio of the machine for each test point wass fixed (as it was determined by the data measured during the test), hence it is logical to see a decrease in the performance of the machine as the molecular weight increases. The above serves to stress the importance of evaluating the performance of centrifugal compressors with an accurate gas composition.

More details concerning the sources of uncertainties for field type tests may be found in the work of Brun and Kurz (2001) and in the Siemens-Energy reference work (2015).

CONCLUDING REMARKS

This paper has offered an overview of the various factors that contribute to the accuracy or lack thereof for centrifugal compressor performance predictions. The primary sources of these errors are in the engineering calculations and/or assumptions, the manufacturing and assembly of the compressor components and the test methods, instrumentation, data reduction, etc. It was also noted that the overall accuracy of the compressor prediction cannot be better than the poorest accuracy of the various contributors. If parts do not match the drawings or solid models, the accuracy of the prediction will suffer. If the test instrumentation uncertainty is too large, it might not be possible to gather data that is accurate enough to determine the true performance of the compressor. If one assumes that the test loop is providing uniform, well-behaved flow to the compressor and it is not, then the test data will not align with the prediction.

The paper highlighted some of the sources of error or uncertainty that can occur during the engineering design process and sited examples of how the manufacturing methods can contribute to inaccuracies in component dimensions. The paper also presented a very detailed description of the methods and instrumentation that are typically used for compressor testing, and identified which parameters have the largest effect on the uncertainty of the derived test data. Sample cases for uncertainty analyses completed on production test stand and field test data were provided for those who wish to delve deeper into the matter.

NOMENCLATURE

Symbols:

d	Orifice throat diameter [in]
D	Pipe internal diameter [in]
DIA	Machine equivalent diameter [in]
DIA_1	Diameter of first impeller [in]
f	Polytropic work factor [-]
g_c	Dimensional constant (32.174) [lbm.ft/lbf.s2]
Fa	Orifice thermal expansion area factor [-]
H	Enthalpy [BTU/lbm]
J	Mechanical equivalent of heat, 778.17 [ft.lbf/BTU]
K_f	Orifice flow coefficient [-]
K_o	Orifice Ko factor [-]
N	Machine speed [rpm]
n	Polytropic volume exponent [-]
n_s	Isentropic volume exponent [-]
P	Pressure [psia]
P_G	Gas power [HP]
P_R	Pressure ratio [-]
Q/N	Volume to speed ratio [ft3/rev]
RPM	Machine rotating speed [rpm]

T	Temperature [°R]
T_R	Temperature ratio [-]
U_2	Impeller tip speed [ft/s]
U_2/A_o	Machine Mach Number [-]
V	Specific volume [ft3/lbm]
V_R	Volume reduction [-]
WF	Mass flow [lbm/min]
W_{in}	Work input coefficient [-]
W_p	Polytropic work [ft.lbf/lbm]
Y_o	Gas expansion factor [-]
β	Diameter ratio of fluid meter (d/D) [-]
ΔP	Pressure drop across orifice [psid]
η_p	Polytropic efficiency [-]
μ_p	Polytropic head coefficient [-]
ρ	Density [lbm/ft3]

Subscripts:

1	Inlet
2	Discharge
3	Discharge (Isentropic Condition)
ori	Upstream of orifice plate
p	Polytropic
s	Isentropic

REFERENCES:

Aikens, K., Sorokes, J., Malinowski, R., Frankzke, A., 2020, "Case Study -- Resolving Centrifugal Compressor Aerodynamic-Performance Issues Related to Inlet Flow Distortion," Proceedings of the 49th Turbomachinery & 36th Pump Symposia, Texas A&M,.

ASME, 1971, PTC 19.5, "Fluid Meters, Part 2", ASME Press.

ASME, 1979, PTC 19.3, "Temperature Measurement", ASME Press.

ASME, 1987, PTC 19.2, "Pressure Measurement", ASME Press.

ASME, 1997, PTC 10, Performance Test Code on Compressors and Exhausters", ASME Press.

ASME, 1998, PTC 19.1 "Test Uncertainty, Instruments and Apparatus", ASME Press

Aungier R. H., 2000, "Centrifugal Compressors: A Strategy for Aerodynamic Design and Analysis", ASME Press.

Benvenuti, E., 1978, "Aerodynamic Development of Stages for Industrial Centrifugal Compressors. Part 1: Testing Requirements and Equipment – Immediate Experimental Evidence", ASME paper 78-GT-4

Borer, C., Sorokes, J. M., McMahon, T., and Abraham, E., 1997, "An Assessment of the Forces Acting Upon a Centrifugal Impeller Using Full Load, Full Pressure Hydrocarbon Testing", Proceedings of the 26th Turbomachinery Symposium, Texas A&M, pp. 111-121, (https://oaktrust.library.tamu.edu/handle/1969.1/163428)

Brun, K., and Kurz, R., 2001, "Measurement Uncertainties Encountered During Gas Turbine Driven Compressor Field Testing", ASME Journal of Engineering for Gas Turbines and Power, Vol. 123, pp. 62-69, New York.

Cave, M. and Ji, M., 2017, "Impeller Manufacturing – Design for Machining," ASME Paper No GT2017-64724.

Childs, P. and Noronha, M., 1997, "The Impact of Machining Techniques on Centrifugal Compressor Impeller Performance," ASME Paper No. 97-GT-456.

Colby, G. M., 2005, "Hydraulic Shop Performance Testing of Centrifugal Compressors," Turbomachinery Symposium Proceedings, Texas A&M, (https://oaktrust.library.tamu.edu/handle/1969.1/163222)

Coleman, H. W., Steele, W. G., 1998, "Experimentation and Uncertainty Analysis for Engineers", John Wiley & Sons, New York.

Cousins, W., Yu, L., Garofano, J., Botros, B., Sishtla, V. and Sharma, O., 2014, "Test and Simulation of the Effects of Surface Roughness on a Shrouded Centrifugal Impeller," ASME Paper No. GT2014-25480.

Crouse, J.E., Sorokes, J.M., 1990. "An Interactive System to Integrate the Design, Analysis, and Manufacture of Centrifugal Compressor Impellers," ASME paper no. 90-GT-230.

Denton, J. D., 2010, "Some Limitations of Turbomachinery CFD", Proc. of ASME Turbo Expo 2010, GT2010-22540.

Dieter, W., 2002, "An Optimized Pneumatic Probe for Investigation of Gas Turbine Aerodynamics in full Scale Gas Turbines", ASME Paper GT-2002-30044.

Durbin, P. A., 2018, "Some Recent Developments in Turbulence Closure Modeling", Annu. Rev. Fluid Mech., 50, pp. 77-103.

Eckardt, D., 1986, "Advanced Experimental Techniques for Turbomachinery Development", Chapter 1 of Principal Lecture Series No. 1 – Advanced Experimental Techniques in Turbomachinery, Concepts ETI, Edited by D. Japikse, Vermont, pp. 1-1 through 1-51.

Frier, S., Burkardt, N., Sorokes, J., "Impeller Manufacturing – Understanding the Methods & Their Impact on Performance," Turbomachinery Symposium Proceedings, Texas A&M, 2020

Gilarranz, J. L., Ranz, A. J., Kopko, J. A., and Sorokes, J. M., 2005, "On the Use of 5-Hole Probes in the Testing of Industrial Centrifugal Compressors", ASME Journal of Turbomachinery, Vol. 127, pp. 91-106.

Gilarranz, J. L., 2005, "Uncertainty Analysis of a Polytropic Compression Process and Application to Centrifugal Compressor Performance Testing", Paper GT-2005-68381, Proceedings of the IGTI/ASME Turbo Expo 2005, Reno, USA.

Gilarranz, J. L., 2006, "Uncertainty Analysis of Centrifugal Compressor Aero-Performance Test Data: Effects of Correlated Systematic Error", Paper GT-2006-90955, Proceedings of the IGTI/ASME Turbo Expo 2006, Barcelona, Spain

Grosso, G., 2020, "Performance Test Procedure", Dresser-Rand Internal Specification Number 003-085-001, Revision 5, Dresser-Rand, Olean.

ISO, 1992, ISO 5389, "Turbocompressors – Performance Test Code", ISO Press.

ISO, 1993, "Guide to the Expression of Uncertainty in Measurements", ISO Press, Geneva.

Japikse, D., 1996, "Centrifugal Compressor Design and Performance", Concepts ETI, Inc.

Kline and McClintock, F. A., 1953, "Describing Uncertainties in Single –Sample Experiments", Mechanical Engineering, Vol. 75, pp. 3 – 8.

Kocur, J., Sorokes, J., Colby, G., Keim, N., 2019, "A Comparison of Type 1 Versus Type 2 Testing – Recent Experiences Testing a High-Pressure, Re-Injection Centrifugal Compressor," Turbomachinery Symposium Proceedings, Texas A&M (https://oaktrust.library.tamu.edu/handle/1969.1/188621)

Kotliar, M., Engstrom, R., and Giachi, M., 1999, "The Use of Computational Fluid Dynamics and Scale Model Component Testing for a Large FCC Prototype Air Compressor", Proceedings of the 28th Turbomachinery Symposium, Texas A&M, pp. 69-76.

Mangani, L., and Mauri, S., 2011, "Assessment of Various Turbulence Models in a High Pressure Ratio Centrifugal Compressor With an Object Oriented CFD Code," ASME Paper No. GT2011-46829.

Moffat, R. J., 1982, "Contributions to the Theory of Single-Sample Uncertainty Analysis", ASME Journal of Fluids Engineering, Vol. 104, pp. 250-260, New York.

Peng, S., Li, T., Wang, X., Dong, M., Liu, Z, Shi, J. and Zhang, H., 2017, "Toward a Sustainable Impeller Production - Environmental Impact Comparison of Different Impeller Manufacturing Methods," Journal of Industrial Ecology, Wiley Periodicals, Inc.

Roduner, C., Köppel, Kupferschmied, P., and Gyarmathy, G., 1998, "Comparison of Measurement Data at the Impeller Exit of a Centrifugal Compressor Measured with Both Pneumatic and Fast-Response Probes", ASME Paper 98-GT-241

Sandberg, M., 2005, "Equation Of State Influences On Compressor Performance Determination," Proceedings of the 34th Turbomachinery Symposium, Texas A&M, pp. 121-129 (https://oaktrust.library.tamu.edu/handle/1969.1/163234)

Saravanamutto, H. I. H., 1990, "Recommended Practices for Measurement of Gas Path Pressures and Temperatures for Performance Assessment of Aircraft Turbine Engines and Components", AGARD Advisory Report No. 245, pp. 77-102.

Schultz, J. M., 1962, "The Polytropic Analysis of Centrifugal Compressors", ASME Journal of Engineering for Power, Vol. 84, pp.69-82, New York.

Siemens Energy, 2015, "Evaluation of Test Uncertainties for Compressor Performance Tests", Siemens Energy Internal Specification Number GER 0196, Siemens Energy, Mount Vernon.

Singh, A. P., Medida, S., Duraisamy, K., 2017, "Machine-Learning-Augmented Predictive Modeling of Turbulent Separated Flows over Airfoils", AIAA Journal, 55 (7

Smout, P. D., 1996, "Temperature Measurements: Probe Installation and Design Criteria", Lecture Series 1996-07 – Temperature Measurements, von Karman Institute for Fluid Dynamics, Edited by T. Arts, Rhode Saint Genese, Belgium.

Smout, P. D., and Ivey, P. C., 1997, Investigation of Wedge Probe Wall Proximity Effects: Part 1- Experimental Study", Journal of Engineering for Gas Turbines and Power, 119, pp. 598-604.

Sorokes, J. M. , and Welch, J. P., 1991, "Centrifugal Compressor Performance Enhancement Through the Use of Single-Stage Development Rig", Proceedings of the 20th Turbomachinery Symposium, Texas A&M, pp. 101-112 (https://oaktrust.library.tamu.edu/handle/1969.1/163540)

Sorokes, J.M., and Welch, J. P., 1992, "Experimental Results on a Rotatable Low Solidity Vaned Diffuser", ASME Paper 92-GT-19.

Sorokes, J. M., and Koch J. M., 1996, "The Use of Single and Multi-Stage Test Vehicles in the Development of the Dresser-Rand DATUM Compressor", Dresser-Rand Technology Journal, 2, pp. 133-147.

Sorokes, J., Soulas, T., Koch, J., and Gilarranz, J. L., 2009, "Full-Scale Aerodynamic and Rotordynamic Testing for Large Centrifugal Compressors", Proceedings of the 38th Turbomachinery Symposium, pp. 71-79, Houston, USA

Sorokes, J., Hardin, J., and Hutchinson, B., 2016, "A CFD Primer – What Do All of Those Colors Really Mean", Texas A&M TurboPump Symposium (https://oaktrust.library.tamu.edu/handle/1969.1/166790)

Sorokes, J., Kuzdzal, M., Peer, D., Lupkes, K., Saretto, S., Srinivasan, R., 2017, "Design and Testing of a High-Pressure-Ratio Centrifugal Stage – Probing the Aerodynamic & Mechanical Limits," Turbomachinery Symposium Proceedings, Texas A&M, 2017 (https://oaktrust.library.tamu.edu/handle/1969.1/166808)

Sorokes, J., and Kuzdzal, M., 2020, "A Review of Aerodynamically Induced Forces Acting on Centrifugal Compressors, and Resulting Vibration Characteristics of Rotors," Proceedings of the 49th Turbomachinery Symposium (https://oaktrust.library.tamu.edu/handle/1969.1/175014).

Verein Deutscher Ingenieure, 1993, VDI 2045 Parts 1 & 2, "Acceptance and Performance Tests on Turbo Compressors and Displacement Compressors", VDI Press.

ACKNOWLEDGEMENT

The authors thank their various colleagues at Siemens-Energy (and Dresser-Rand) for their help in assembling the information needed for this paper. In particular, we thank Mr. Charles Dunn and Mr. Andrew Ranz for their much-needed assistance. Finally, we thank Siemens-Energy for allowing us to publish this work and the Texas A&M Turbomachinery Laboratory for organizing the excellent venue for presenting this work.